

DIRECT Distances to Nearby Galaxies Using Detached Eclipsing Binaries and Cepheids. VII. Additional Variables in the Field M33A Discovered with Image Subtraction¹

B. J. Mochejska, J. Kaluzny

Copernicus Astronomical Center, Bartycka 18, 00-716 Warszawa

e-mail: mochejsk@camk.edu.pl, jka@camk.edu.pl

K. Z. Stanek², D. D. Sasselov³ & A. H. Szentgyorgyi

Harvard-Smithsonian Center for Astrophysics, 60 Garden St., Cambridge, MA 02138

e-mail: kstanek@cfa.harvard.edu, sasselov@cfa.harvard.edu
aszentgyorgyi@cfa.harvard.edu

ABSTRACT

DIRECT is a project to obtain directly the distances to two Local Group galaxies, M31 and M33, which occupy a crucial position near the bottom of the cosmological distance ladder.

As the first step of the DIRECT project we have searched for detached eclipsing binaries (DEBs) and new Cepheids in the M31 and M33 galaxies with 1m-class telescopes. In this seventh paper we present a catalog of variable stars discovered in the data from the followup observations of DEB system D33J013346.2+304439.9 in field M33A $[(\alpha, \delta) = (23^\circ 55, 30^\circ 72), \text{J}2000.0]$, collected with the Kitt Peak National Observatory 2.1m telescope. In our search covering an area of $108''^2$ we have found 434 variable stars: 63 eclipsing binaries, 305 Cepheids, and 66 other periodic, possible long period or non-periodic variables. Of these variables 280 are newly discovered, mainly short-period and/or faint Cepheids. Their light curves were extracted using the ISIS image subtraction package. For 85% of the variables we present light curves in standard *V* and *B* magnitudes, with the remaining 15% expressed in units of differential flux.

We have discovered a population of first overtone Cepheid candidates and for eight of them we present strong arguments in favor of this interpretation.

We also report on the detection of a non-linearity in the KPNO T2KA and T1KA cameras.

The catalog of variables, as well as their photometry (about 7.8×10^4 BV measurements) and finding charts, is available electronically via anonymous ftp and the World Wide Web. The complete set of the CCD frames is available upon request.

¹Based on observations obtained with the 2.1m telescope at the Kitt Peak National Observatory.

²Hubble Fellow.

³Alfred P. Sloan Research Fellow.

1. Introduction

Starting in 1996 we undertook a long term project, DIRECT (i.e. “direct distances”), to obtain the distances to two important galaxies in the cosmological distance ladder, M31 and M33. These “direct” distances will be obtained by determining the distance of Cepheids using the Baade-Wesselink method and by measuring the absolute distance to detached eclipsing binaries (DEBs). While the cosmological distance scale has been the subject of numerous recent observation campaigns, especially those enabled by the Hubble Space Telescope (HST) and massive variability studies of the Magellanic clouds, M33 has not been re-surveyed since the photographic survey of Kinman, Mould & Wood (1987).

M31 and M33 are the stepping stones to most of our current effort to understand the evolving universe at large scales. First, they are essential to the calibration of the extragalactic distance scale. Second, they constrain population synthesis models for early galaxy formation and evolution and provide the stellar luminosity calibration. There is one simple requirement for all this—accurate distances. These distances are now known to no better than 10-15%, as there are discrepancies of 0.2 – 0.3 mag between various distance indicators (e.g. Huterer, Sasselov & Schechter 1995; Holland 1998; Stanek & Garnavich 1998).

DEBs have the potential to establish distances to M31 and M33 with an unprecedented accuracy of better than 5% and possibly to better than 1%. Detached eclipsing binaries (for reviews see Andersen 1991; Paczyński 1997) offer a single step distance determination to nearby galaxies and may therefore provide an accurate zero point calibration of various distance indicators – a major step towards very accurate determination of the Hubble constant, presently an important but daunting problem for astrophysicists. DEBs have been recently used to obtain accurate distance estimate to the Large Magellanic Cloud (e.g. Guinan et al. 1998; Udalski et al. 1998).

The detached eclipsing binaries have yet to be used as distance indicators to M31 and M33. According to Hilditch (1996) there was only *one* eclipsing binary of any kind known in M33 (Hubble 1926). The recent availability of large-format CCD detectors and inexpensive CPUs has made it possible to organize a massive search for periodic variables, which will produce a handful of good DEB candidates. These can then be spectroscopically followed-up with the powerful new 6.5-10 meter telescopes.

The study of Cepheids in M33 has a venerable history (Hubble 1926). Freedman, Wilson & Madore (1991) obtained multi-band CCD photometry of some of the Cepheids discovered in photographic surveys, to build a period-luminosity relations in M33. However, the sparse photometry and the small sample (11 Cepheids) do not provide a good basis for obtaining direct Baade-Wesselink distances (see, e.g., Krockenberger, Sasselov & Noyes 1997) to Cepheids—the need for new digital photometry has been long overdue.

As the first step of the DIRECT project we have searched for DEBs and new Cepheids in the M31 and M33 galaxies. We have analyzed five $11' \times 11'$ fields in M31, A-D and F (Kaluzny et al.

1998, 1999; Mochejska et al. 1999; Stanek et al. 1998, 1999; hereafter Papers I, IV, V, II, III). A total of 410 variables, mostly new, were found: 48 eclipsing binaries, 206 Cepheids and 156 other periodic, possible long-period or non-periodic variables. We have also analyzed two fields in M33, A and B (Macri et al. 2001a; hereafter Paper VI) and found 544 variables: 47 eclipsing binaries, 251 Cepheids and 246 other variables.

As a second step, we started followup observations of selected DEBs in both the M31 and M33 galaxies with bigger telescopes in order to construct more precise and well sampled light curves for them.

In this paper, seventh in the series, we present a catalog of variable stars found in the same field as the detached eclipsing binary D33J013346.2+304439.9 using followup observations collected at the Kitt Peak National Observatory 2.1m telescope. The paper is organized as follows: Section 2 provides a description of the observations. The data reduction procedure is outlined in Section 3. The catalog of variable stars is presented in Section 4, followed by its brief discussion in Section 5. Section 6 deals with the first overtone Cepheid candidates. The concluding remarks are stated in Section 7.

2. Observations

The data discussed in this paper was obtained at the Kitt Peak National Observatory⁴ 2.1m telescope equipped with a Tektronix 2048×2048 CCD (T2KA camera) having a pixel scale $0.305''/\text{pixel}$ during two separate runs, from September 29th to October 5th, 1999 and from November 1st to 7th, 1999. The primary observing targets were three detached eclipsing binaries, one in each of the fields M33A, M33B and M31A, discovered previously as part of the DIRECT project (Papers VI and II). For field M33A we collected $158 \times 600s$ exposures in the V filter and $62 \times 600s$ in the B filter.⁵ The exposure times varied slightly to compensate for the changes of seeing conditions. The typical seeing was $1''.4$. The field was observed through airmass ranging from 1 to 1.9, with the average at 1.2. The completeness of our data starts to drop rapidly at about 21.2 mag in V and 21.8 mag in B , judging from the magnitude distributions of the variable stars (Fig. 1).

⁴Kitt Peak National Observatory is a division of NOAO, which are operated by the Association of Universities for Research in Astronomy, Inc. under cooperative agreement with the National Science Foundation.

⁵The complete list of exposures for this field and related data files are available through anonymous ftp on `cfa-ftp.harvard.edu`, in `pub/kstanek/DIRECT` directory. Please retrieve the `README` file for instructions. Additional information on the DIRECT project is available through the WWW at <http://cfa-www.harvard.edu/~kstanek/DIRECT/>.

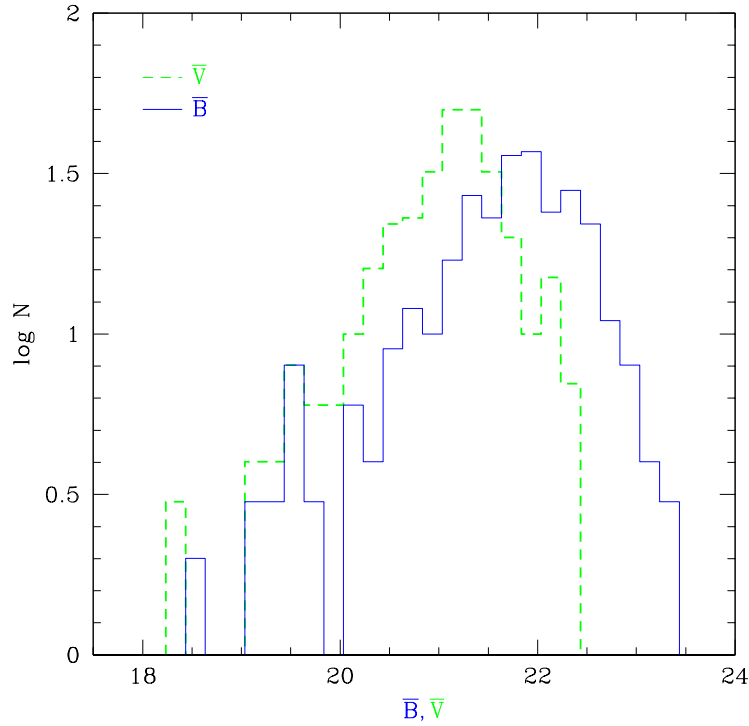


Fig. 1.— Distributions in B (continuous line) and V (dashed line) of variable stars in the field M33A.

3. Data reduction

3.1. Correction for the non-linearity of the T2KA camera

During the second night of the first observing run we compared the photometry from two images of NGC 7789 with differing exposure times and found that the camera had a non-linear response. To lessen the impact of non-linearity we reduced the gain setting from 5.1 to 3.6 e^-/ADU .

Several sets of calibration frames were collected at both gain settings for the purpose of correcting the data for the non-linearity. Each set consisted of a series of dome flats with intensities from ~ 500 ADU to ~ 60000 ADU. After subtracting the readout bias under IRAF⁶ the mode intensity I_i (in ADU) was computed for each calibration frame.

We adopted the correction function for the non-linearity in the same form as in the IRAF task IRLINCOR:

$$I_e = I_i \cdot (c_1 + c_2 \cdot \frac{I_i}{32767} + c_3 \cdot (\frac{I_i}{32767})^2) \quad (1)$$

⁶IRAF is distributed by the National Optical Astronomy Observatories, which are operated by the Association of Universities for Research in Astronomy, Inc., under cooperative agreement with the NSF.

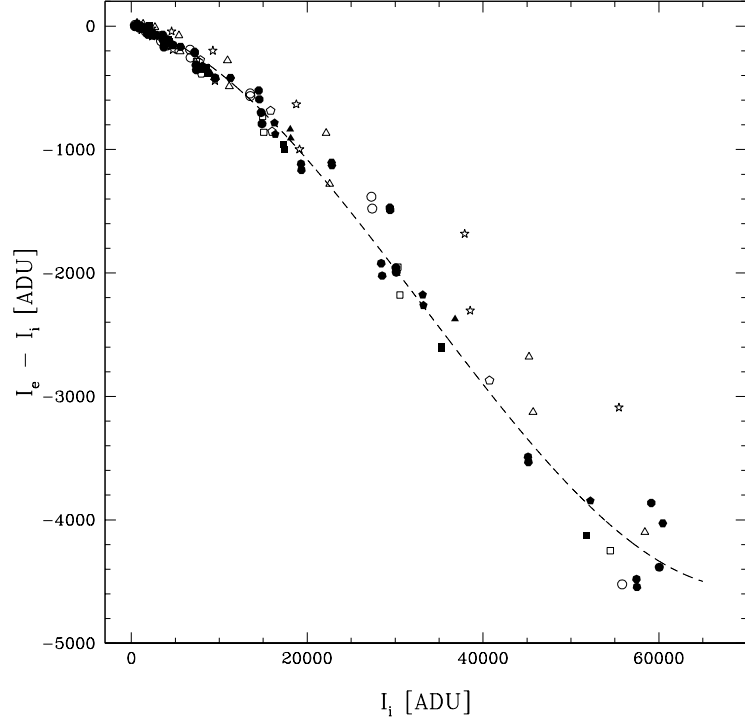


Fig. 2.— The difference between the expected intensity I_e and the measured intensity I_i as a function of the measured intensity. Each point corresponds to a calibration exposure. Exposures from the same set are marked with like symbols. Only the points indicated by filled symbols were used to fit the correction function (dashed line).

where I_i is the mode observed intensity on the calibration frame, I_e the intensity corrected to the expected level and the coefficients c_1, c_2, c_3 are to be determined. The exposure time, t corrected for the shutter speed (0.1 s), was used to calculate the expected intensity I_e from the measured intensity level I_i :

$$I_e = I_i \cdot \frac{t}{t_0}$$

By definition the detector response was assumed to be linear at the intensity level of the image with the shortest exposure time t_0 . The coefficients c_1, c_2 and c_3 were determined from a least-squares fit of Eq. 1 to the measured and expected intensity levels I_i and I_e . We list them in Tab. 1 for the two gain settings used.

Figure 2 shows the difference between the expected intensity I_e and the measured intensity I_i as a function of the measured intensity for gain $3.6e^-/\text{ADU}$. Each point corresponds to a calibration exposure. Exposures from the same set are marked with like symbols. The points exhibit substantial scatter between the sets and in some cases within the set (ie. open stars and open triangles). Several fits were made to different combinations of sets. The derived coefficients were then tested on pairs of frames of the same object with exposure times differing by a factor of

at least 10. The fit corresponding to the best coefficients is shown with a dotted line on Fig. 2. The calibration frames used in the fit are indicated by filled symbols.

A comparison between the photometry derived from a 100s and a 10s exposure of the NGC 7789 open cluster is presented in Fig.3. The left panel shows a comparison for the uncorrected exposures and the right panel for the corrected ones. A significant improvement is seen between the uncorrected and corrected frames. A close inspection of the right panel of the figure will reveal that the non-linearity has not been removed completely.

The standard preliminary processing of the science data was performed with the routines in the IRAF CCDPROC package. The non-linearity was corrected with the IRLINCOR task using the derived coefficients.

3.2. Nonlinearity of the T1KA CCD

During an observing run in October 1998 at the KPNO 2.1 meter telescope we have collected data using the T1KA 1024×1024 CCD. We have compared a series of images of an open cluster, Be 32, which were obtained one after another in photometric conditions (Fig. 4). The images vary only in exposure times (starting at 6 seconds and going up to 180 seconds). We have found that the magnitudes (obtained via point spread function fitting + aperture correction) do not differ by the expected factor of $2.5 \log(\text{time})$, but rather show increasing deviations from the expected scaling as the difference in exposure time gets larger. Furthermore, the relations show strong non-linearity, which increases with the difference in exposure time. This fact was not known to us during the time of observations and no calibration frames were collected to correct the data. We provide this information to warn the astronomical community of the problem we have encountered with this camera.

Table 1. COEFFICIENTS FOR THE NON-LINEARITY
CORRECTION FUNCTION

gain (e^-/ADU)	c_1	c_2	c_3
3.6	0.983282	-0.0765595	0.0252555
5.1	0.967008	-0.0354981	-0.0314427

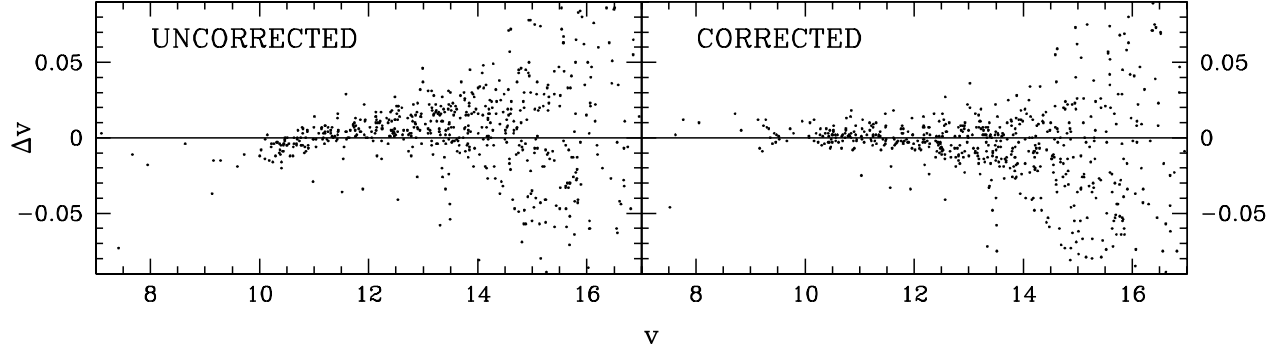


Fig. 3.— A comparison between the T2KA photometry obtained from a 100s and a 10s exposure of the open cluster NGC 7789. Left panel: No correction was applied. Right panel: The exposures were corrected with a third order polynomial.

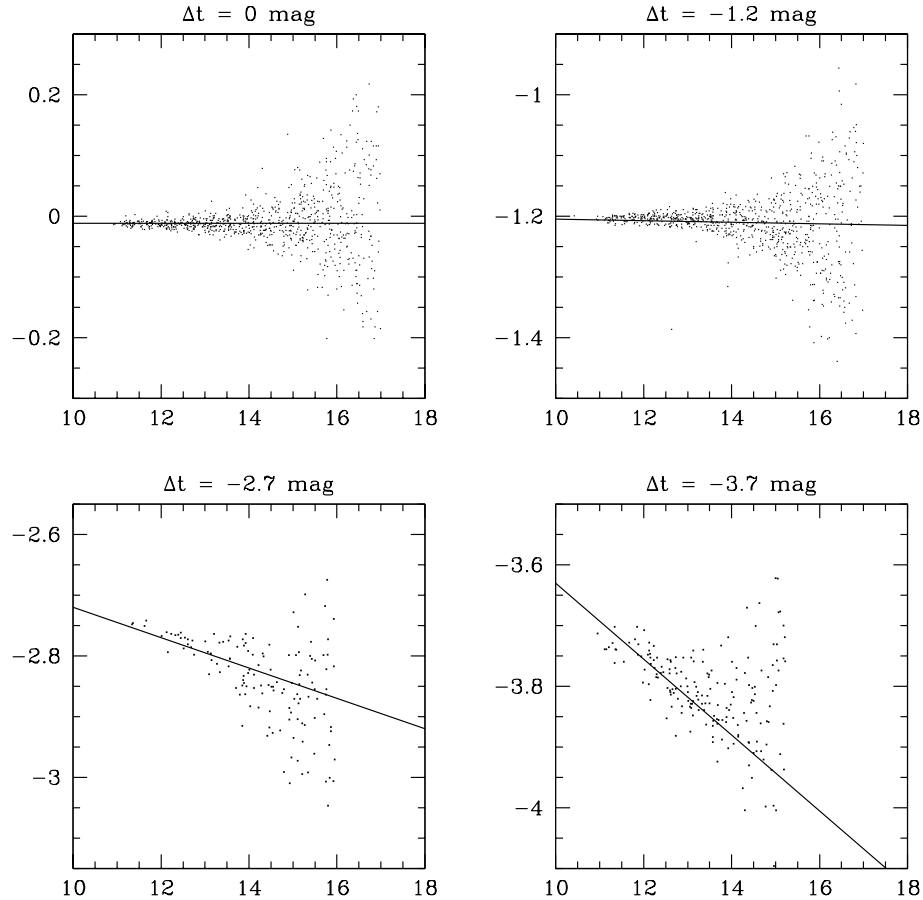


Fig. 4.— A comparison between the T1KA photometry of the open cluster Be 32 obtained from exposures of varying lengths. Going from the upper left to the lower right panel the photometry from a 180 s exposure is compared with that of: 180 s, 60 s, 15 s and 6 s.

3.3. Photometry and Selection of Variables

The photometry for the variable stars was extracted using the ISIS image subtraction package (Alard & Lupton 1998, Alard 2000a) from the *V* and *B*-band data.

The ISIS reduction procedure consists of several steps. Initially all of the frames are transformed to a common coordinate grid. Next a reference image is created by stacking several frames with the best seeing. For each frame the reference image is convoluted with a kernel to match its point spread function (PSF) and then subtracted. On the subtracted images the constant stars will cancel out and only the signal from variable stars should remain. A median image is constructed of all the subtracted images and the variable stars are identified as bright peaks on it. Finally, profile photometry is extracted from the subtracted images.

All of the computations were performed with the frames internally subdivided into four sections (the ISIS parameters `sub_x` and `sub_y` set to 2). The differential brightness variations of the background were fit with a second degree polynomial (`deg_bg=2`). A convolution kernel varying quadratically with position was chosen (`deg_spatial=2`).

An image of particularly good quality was selected as the template frame for the stellar positions. The remaining images were re-mapped to the template frame coordinate system using a third degree polynomial transform. During this step an initial rejection of cosmic rays was also performed. A setting of 1.0 for the cosmic ray threshold (`COSMIC_THRESH`) was used.

A reference image was then constructed from 25 images with the best seeing. The minimum, maximum and average seeing of these 25 images were 0.95'', 1.23'' and 1.11'' in *V* and 0.93'', 1.28'' and 1.13'' in *B*. The constituent images were transformed to the same seeing and background level as the best image (the template in our case) and stacked by taking a median in each pixel to obtain the reference image virtually free of cosmic rays.

Image subtraction was then applied to all the frames. For each frame the reference image was convoluted with a kernel to match it as closely as possible and then the frame was subtracted from it. As the flux of the non-variable stars on both images should be almost identical, such objects will disappear from the subtracted image. The only remaining signal will come from variable stars.

To obtain a better signal-to-noise ratio a median of the subtracted images was computed for the purpose of detecting variable stars. The variables were then identified as bright peaks on this image. In practice the situation is slightly complicated by the presence of stars saturated on the reference image, as their profiles were not matched exactly to those on frames with inferior seeing. An easy way to distinguish genuine variables from saturated stars is by their profile on the subtracted image: it should be smooth for the variables and usually contains a flat top or a dip at the center for the saturated stars. The variables were identified visually on the median subtracted image and their positions recorded with the IMEXAMINE task under IRAF. The final positions were derived with the DAOPHOT FIND subroutine (Stetson 1987). Variables were identified in both bands. The lists were then merged into a master variable list.

The light curves of the variables (in ADU) were extracted from the subtracted images. Preliminary periods were found with the ISIS *czerny* subroutine, based on the analysis of variance method, as described by Schwarzenberg-Czerny (1989), and later refined using the same algorithm. Stars with chaotic and/or noisy light curves were rejected from the sample upon visual inspection.

In the next step the light curves were converted into magnitudes. PSF-fitting photometry was extracted with the DAOPHOT/ALLSTAR package from the template image following the approach described in Paper I. Some of the variable stars were not detected on the template, in most cases because of their faintness or crowding. As light curves of these stars could not be converted to magnitudes, they were left expressed in counts.

The template instrumental magnitude m_{tpl} of each variable was converted into counts c_{tpl} , using the ALLSTAR zeropoint of 25 mag. The light curve was then converted point by point to magnitudes m_i , by computing the total flux c_i for the given epoch as the sum of the counts on the template c_{tpl} and the counts on the subtracted template image $\Delta c_{tpl} = c_{ref} - c_{tpl}$ decreased by the counts corresponding to the subtracted image $\Delta c_i = c_{ref} - c_i$.

$$c_i = c_{tpl} + \Delta c_{tpl} - \Delta c_i \quad (2)$$

The flux was converted to instrumental magnitudes, using the same zero point as above. To convert the photometric error $\sigma_{c,i}$ from counts to $\sigma_{m,i}$ magnitudes, we used the following relation:

$$\sigma_{m,i} = -2.5 \log\left(\frac{c_i}{c_i + \sigma_{c,i}}\right) \quad (3)$$

3.4. Photometric Calibration and Astrometry

On the nights of October 3/4 and November 3/4 1999 we observed a total of 75 stars in 13 Landolt (1992) fields. We attempted to derive a calibration from these exposures, corrected for non-linearity. The o-c residuals showed a clear dependence on magnitude, especially in the V -band, where they exhibited a very similar slope on both nights. Several new fits to Eq. 1 with different combinations of data sets were tried. Those that gave some improvement in the calibration, produced noticeably inferior results when the photometry on two images of very different exposure times was compared. We had decided to stay with the initial values for the correction coefficients (Tab. 1) and calibrate our photometry using a different method. The coefficients for the color terms were derived from the comparison of our NGC 6791 photometry with the data from the KPNO 0.9m telescope (Kaluzny & Udalski 1992). The offsets were determined relative to the DIRECT catalog of stellar objects in M33 (Macri et al. 2001b). The following transformations were adopted:

$$\begin{aligned} v &= V - 5.491 + 0.039 \cdot (B - V) \\ b - v &= 0.178 + 0.927 \cdot (B - V) \\ b &= B - 5.312 - 0.034 \cdot (B - V) \end{aligned}$$

The instrumental V and B -band light curves of the variables were transformed to the standard system by adding the appropriate offsets, as the coefficients next to the color terms are very small.

Equatorial coordinates were determined for the V template star list, expanded with the variables with no V -band photometry. The transformation from rectangular to equatorial coordinates was derived using 818 transformation stars with $V < 19.5$ from the DIRECT catalog of stellar objects in M33 (Macri et al. 2001b). The average difference between the catalog and the computed coordinates for the transformation stars was $0.^{\circ}07$ in right ascension and $0.^{\circ}06$ in declination. As a check we have also obtained an independent transformation to the USNO-A2 catalog (Monet et al. 1996) using 56 transformation stars ($\Delta\alpha = 0.^{\circ}26$, $\Delta\delta = 0.^{\circ}23$). The average differences between the computed coordinates and the M33 catalog for 1334 stars with $V < 19.5$ were $\Delta\alpha = 0.^{\circ}71$ and $\Delta\delta = 0.^{\circ}60$.

4. Catalog of Variables

4.1. Classification

The variables we are most interested in are Cepheids and eclipsing binaries (EBs). We therefore searched our sample of variable stars primarily for these two classes of variables. The variable stars were preliminarily classified as eclipsing, Cepheid or miscellaneous by visual inspection, based on the shape of their light curves. The variables for which neither V nor B -band magnitude could be determined (with only flux light curves or having a period in excess of 14 days) were not reclassified further.

In order to obtain as clean a sample of Cepheids as possible, we have inspected the location of the Cepheid variable candidates on a $V/B - V$ CMD. All of the Cepheid candidates having highly discrepant colors were reclassified as other periodic variables. The candidates with light curves in only one of the bands were checked on the period-luminosity relation for that band. Extreme outliers were also moved to the other periodic variable category.

The EBs with light curves expressed in magnitudes for at least one band, were fitted with a model described in Papers I and II. Within our assumption the light curve of an EB is determined by nine parameters: the period, the zero point of the phase, the eccentricity, the longitude of periastron, the radii of the two stars relative to the binary separation, the inclination angle, the fraction of light coming from the bigger star and the uneclipsed magnitude. Eclipsing binary candidates for which a satisfactory fit was not achieved, were reclassified as other periodic variables.

In the following sections 4.2-4.5 we present the parameters and light curves for the 434 identified variable stars.⁷ All tables are sorted by increasing period, unless otherwise noted. We

⁷The BV photometry and V finding charts for all variables are available from the authors via the `anonymous ftp`

adopt a naming convention after Macri et al. (2001a) based on the J2000.0 equatorial coordinates, in the format: D33J $hhmmss.s$ + $ddmmss.s$. The first three fields ($hhmmss.s$) correspond to right ascension expressed in hours, the last three ($ddmmss.s$) to declination, expressed in degrees, separated by the declination sign. As none of the newly discovered variables are present in previous variable star catalogs, we refer the reader to Tables 5 and 6 in Paper VI for cross-identifications.

4.2. Eclipsing Binaries

We have found a total of 63 eclipsing binaries in field M33A. In Table 2 we present the parameters for the 53 EBs with a magnitude light curve in at least one band. For each variable we list its name, period P , magnitudes V_{max} and B_{max} of the system outside of the eclipse, and the radii of the binary components R_1 , R_2 in the units of the orbital separation. We also give the inclination angle of the binary orbit to the line of sight i and the eccentricity of the orbit e . The reader should bear in mind that the values of V_{max} , B_{max} , R_1 , R_2 , i and e are derived with a straightforward model of the eclipsing system, so they should be treated only as reasonable estimates of the “true” value. Table 3 lists 10 EBs with flux light curves only. For each variable we give its name and period P . Figure 5 presents the phased light curves of 12 sample EBs (see also Table 8).

4.3. Cepheids

A total of 305 Cepheid variables were found in field M33A. In Table 4 we present 242 Cepheids with a magnitude light curve in at least one band. For each variable, we list its name, period P , flux-weighted average magnitudes $\langle V \rangle$ and $\langle B \rangle$ and the V and B -band amplitudes A_V and A_B . Due to the short time base of our observations, reliable flux-weighted magnitudes could only be determined for variables with periods shorter than 14 days. We have extracted light curves for 36 Cepheids with longer periods, all of them identified previously in Paper VI and made them available via `anonymous ftp`. In Table 5 we list 27 Cepheids with flux light curves only. For each variable we list its name and period P . Figure 6 presents the phased light curves of 24 sample Cepheids (see also Table 9).

4.4. Other Periodic Variables

In Table 6 we present the parameters of 13 periodic variables. For each variable we list its name, period P , the magnitudes V and B and the V and B -band amplitudes A_V and A_B . The V and B columns list the magnitudes outside of the eclipses V_{max} and B_{max} for the eclipsing

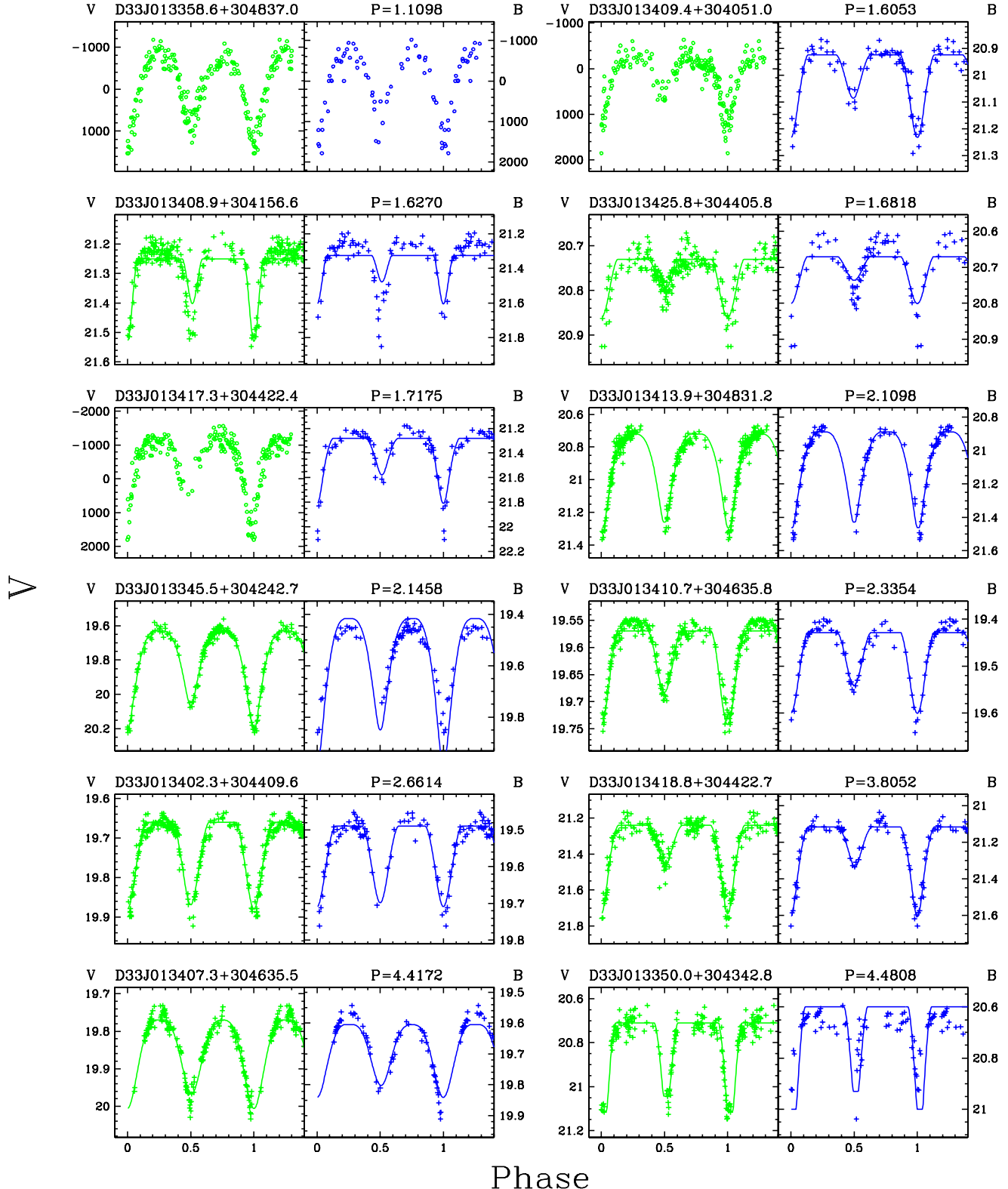


Fig. 5.— Selected BV light curves of eclipsing binaries found in the field M33A. The points on the light curves expressed in magnitudes are marked with crosses, the flux ones by open circles. The thin continuous line represents the best fit model for each star and photometric band.

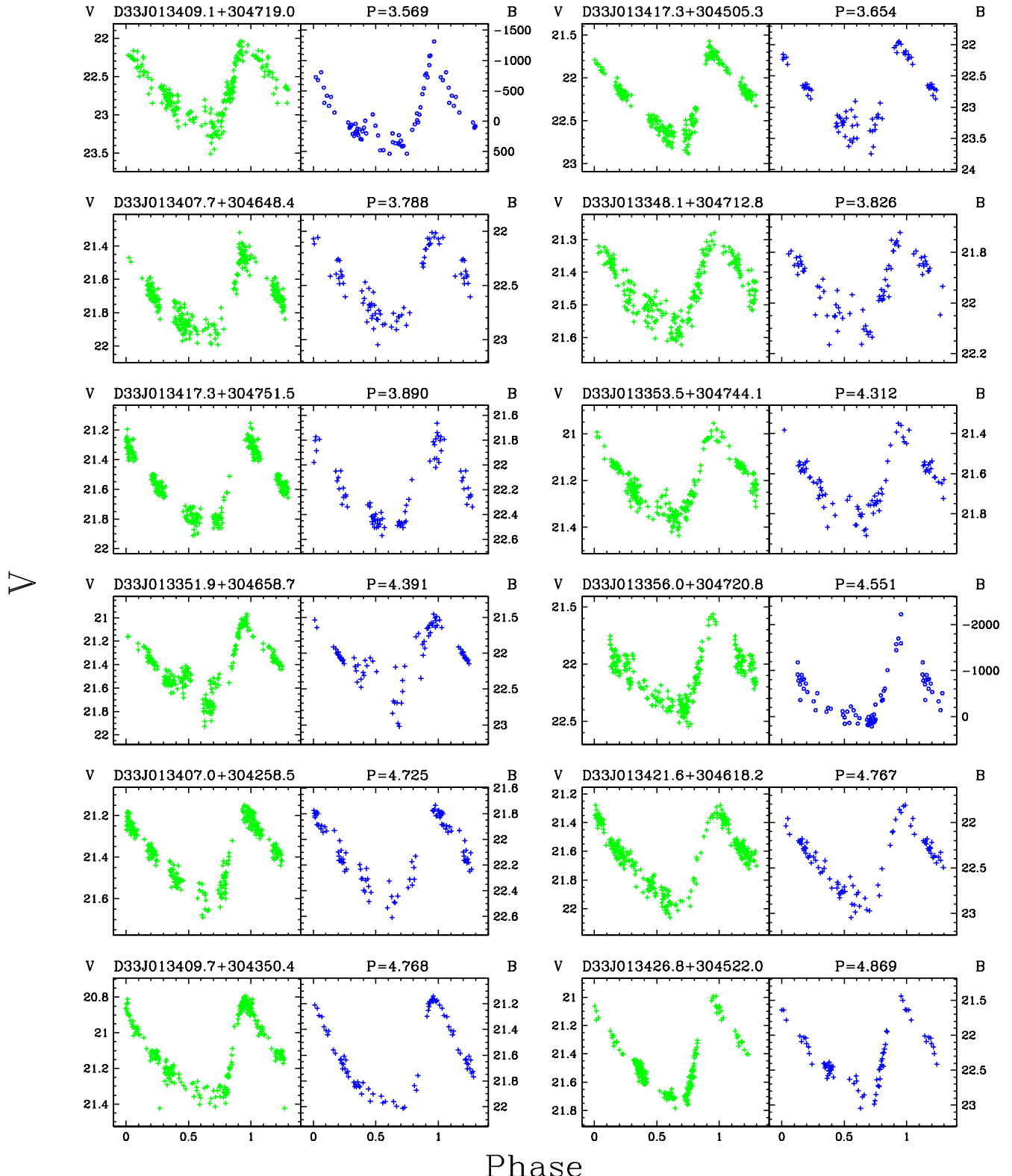


Fig. 6.— Selected *BV* light curves of Cepheid variables found in the field M33A. The points on the light curves expressed in magnitudes are marked with crosses, the flux ones by open circles.

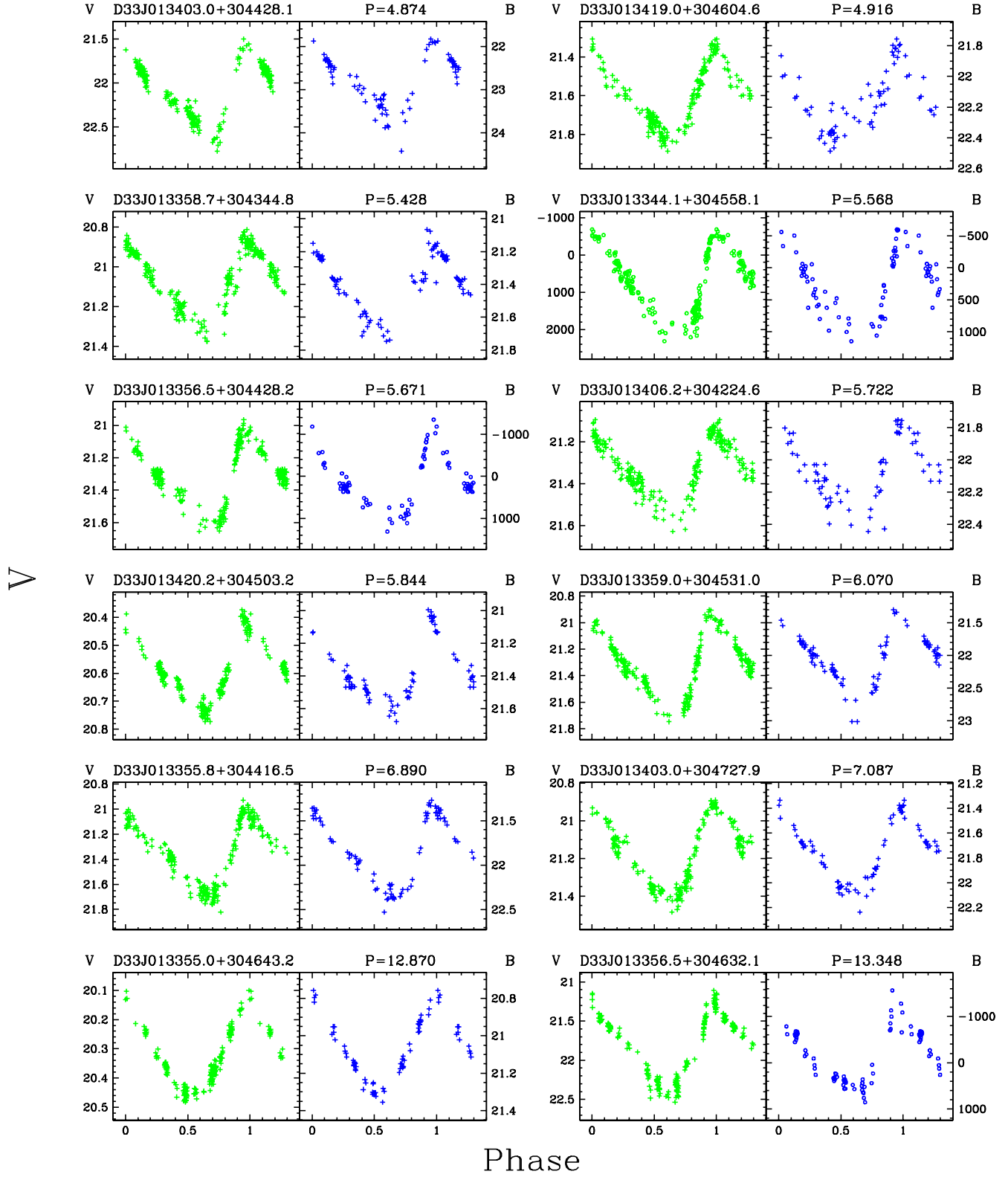


Fig. 6.— Continued.

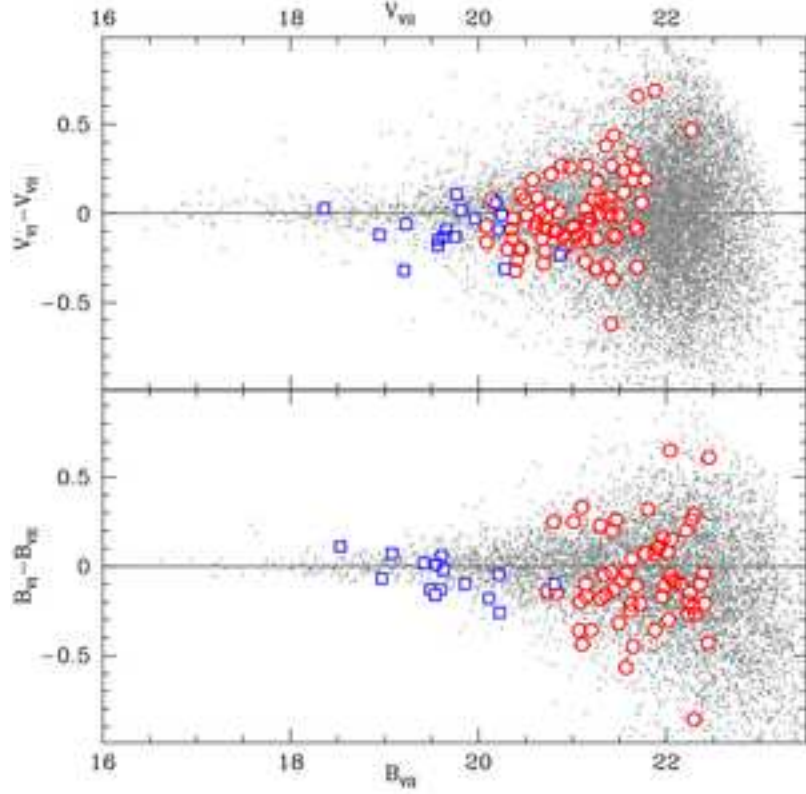


Fig. 7.— A comparison between variable star photometry in the V (upper panel) and B -band (lower panel) between our catalog and Paper VI. EBs are denoted by squares and Cepheids by circles. All other stars in the field are plotted with small dots in the background for reference.

variables and flux-weighted average magnitudes $\langle V \rangle$ and $\langle B \rangle$ for the other variables. We have also found three other variables with periods of the order of 50 days (identified previously in Paper VI), which we do not list in the table. Their light curves are available via `anonymous ftp`. In Table 10 we list the light curves of all periodic variables.

4.5. Miscellaneous Variables

In Table 7 we present the parameters of 50 miscellaneous variables. For each variable we list its name, the average magnitudes \bar{V} and \bar{B} and the V and B -band amplitudes A_V and A_B . Variable D33J013342.3+304024.7 is probably an EB, with incomplete phase coverage. Several of those variables are most likely periodic, with periods in excess of 14 days. In Table 11 we list the light curves of all miscellaneous variables.

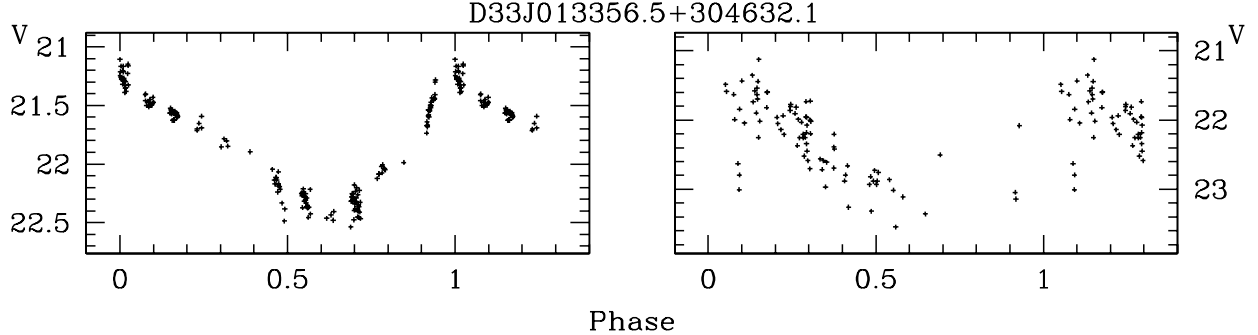


Fig. 8.— A comparison of V -band light curves for the type II Cepheid D33J013356.5+304632.1 ($P=13.348$ days) from our catalog and Paper VI. The ISIS light curve obtained with the 2.1m telescope is shown in the left panel and the DAOPHOT light curve from 1.3m telescope data in the right panel.

4.6. Comparison with the catalog in Paper VI

In Figure 7 we compare our V and/or B photometry for 81 Cepheids (circles) and 18 EBs (squares) with the values listed in the DIRECT catalog of variables in M33 (Paper VI). As reference we plot in the background similar comparisons for all the stars in the field (dots). The variables, with some exceptions, have ΔB and ΔV distributions roughly similar to the rest of the stars, although they do show a marked tendency to be fainter in our catalog. This trend is especially prominent in the V -band for the EBs, but is absent in their B -band comparison. We have examined the images of three of the more discrepant EBs and found that in our data we have resolved more nearby companions to these variables. These companions are brighter in V than in B , relative to the EBs. This is not surprising, as the EBs are among of the bluest stars in the field. There are also a few faint Cepheids, which show unusually large differences in photometry, of the order of 0.6-0.8 mag. We have inspected their light curves in both catalogs. The V -band light curves of one such star, type II Cepheid D33J013356.5+304632.1, are shown in Fig. 8. The left panel shows our light curve, extracted with ISIS from 2.1m telescope data. The right panel shows the DAOPHOT light curve from data taken with a 1.3m telescope (Paper VI). It seems that these discrepancies are caused in large part by the fact that fixed position photometry is prone to identify and fit a profile at the supplied position even when the star is below the detection threshold, resulting in the false measurement of a fainter magnitude.

In Figure 9 we plot a histogram of the surface density of Cepheids (N/kpc^2) as a function of their period, assuming a distance of 840 kpc to M33 (Freedman, Wilson & Madore 1991). The solid line represents all Cepheids from our catalog with $P < 14$ days, the dashed line – the Cepheids from Paper VI. The areas covered in this search and in Paper VI are 108 and 222 arcmin 2 . As our observations were carried out during two one-week runs spaced one month apart, we lack the baseline to detect long period Cepheids. Since our data were collected with an instrument 2.6 times larger in area and with better seeing, we have a higher detection rate for

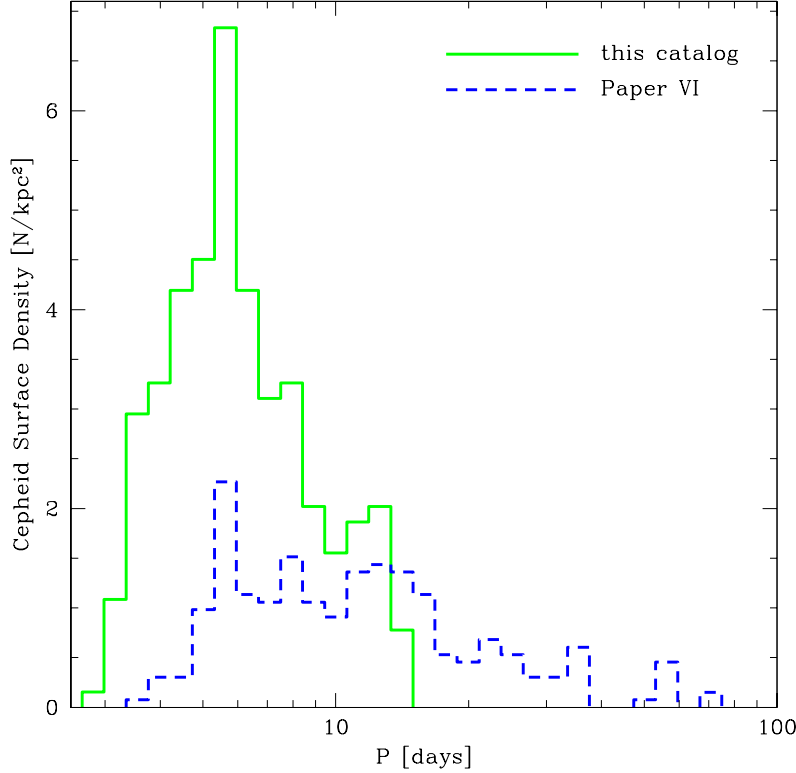


Fig. 9.— A histogram of the surface density of Cepheids (N/arcmin^2) as a function of their period. The solid line represents all Cepheids from our catalog with $P < 14$ days, the dashed line – the Cepheids from Paper VI.

short period Cepheids. The Paper VI catalog, due to the much longer baseline of observations, contains more long period Cepheids.

5. Discussion

In Fig. 10 we plot the positions of the variable stars on the $V/B - V$ CMD. The EBs are denoted by open squares and Cepheids by filled circles in the left panel, the periodic variables by filled squares and miscellaneous by open circles in the right panel.

All of the EBs occupy the upper main sequence, with the exception of D33J013359.5+304037.6 ($B - V = 0.37$). This variable most likely suffers from larger than average reddening, as it is located at the edge of what appears to be a dust lane.

Most Cepheids occupy the region between $0.3 < B - V < 1.0$, with several outliers stretching from $B - V = 0.10$ to $B - V = 1.24$. The discrepant colors of some of the Cepheid variables most likely originate from the phenomenon of blending with nearby bright stars of very different colors

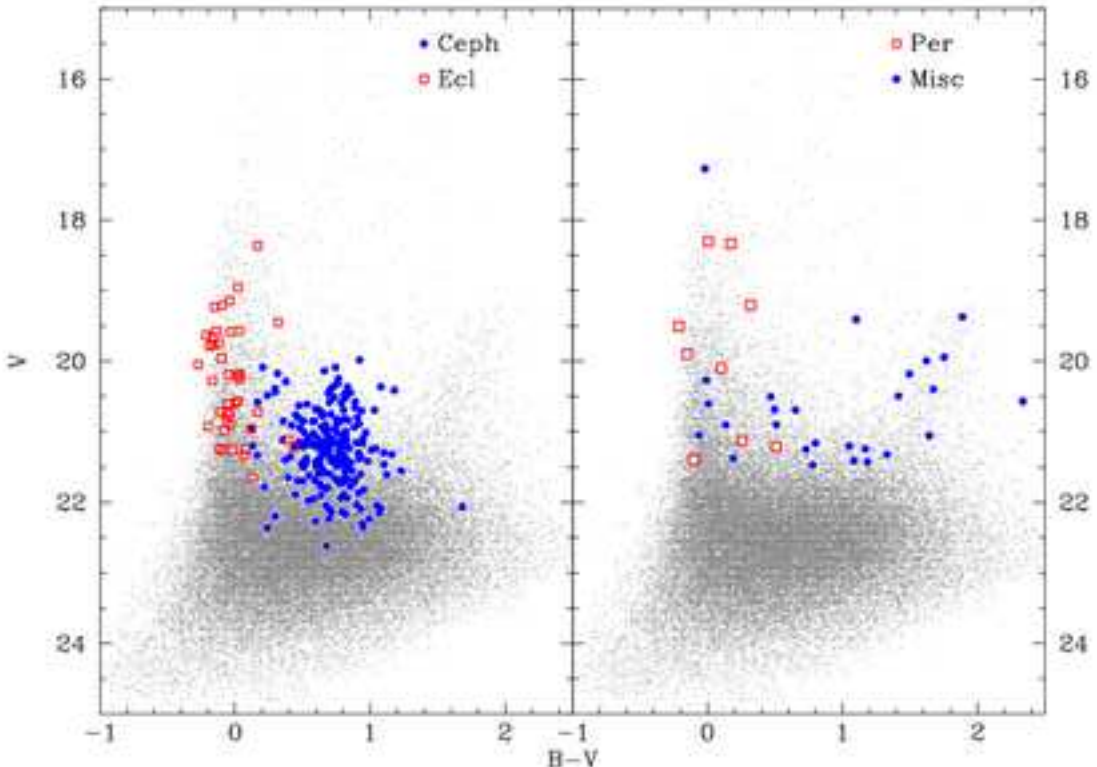


Fig. 10.— The $V/B - V$ CMD for the variable stars in field M33A. The EBs (open squares) and Cepheids (filled circles) are shown in the left panel, periodic (filled squares) and miscellaneous variables (open circles) in the right panel.

and/or reddening. The phenomenon of blending occurs when the Cepheid possesses one or more close companions which cannot be separated at the resolving power of the instrument used. A further discussion of blending and its properties can be found in Mochejska et al. (2000; 2001) and Stanek & Udalski (1999).

All but one of the periodic variables with BV photometry are bluer than $B - V = 0.35$. The five brightest ones exhibit Cepheid-like light curves of very low amplitude of the order of a few hundredths of a magnitude. The low amplitudes of their variability suggest that these could be Cepheids blended with blue main sequence stars. The remaining four periodic variables are likely EBs. Three of them have blue colors, consistent with this type of variable. The fourth one, D33J013346.1+304658.9, with a period of 6.4640 days seems to be a contact EB, despite its unusual color ($B - V = 0.511$). A more complete light curve would be required to resolve the true nature of this object.

The miscellaneous variables are spread throughout the CMD. Some are located on the upper main sequence, and a few seem to fall on the upper red giant branch. Several seem to occupy the same region as Cepheids. It is possible that some of these variables are Cepheids with periods in excess of 14 days.

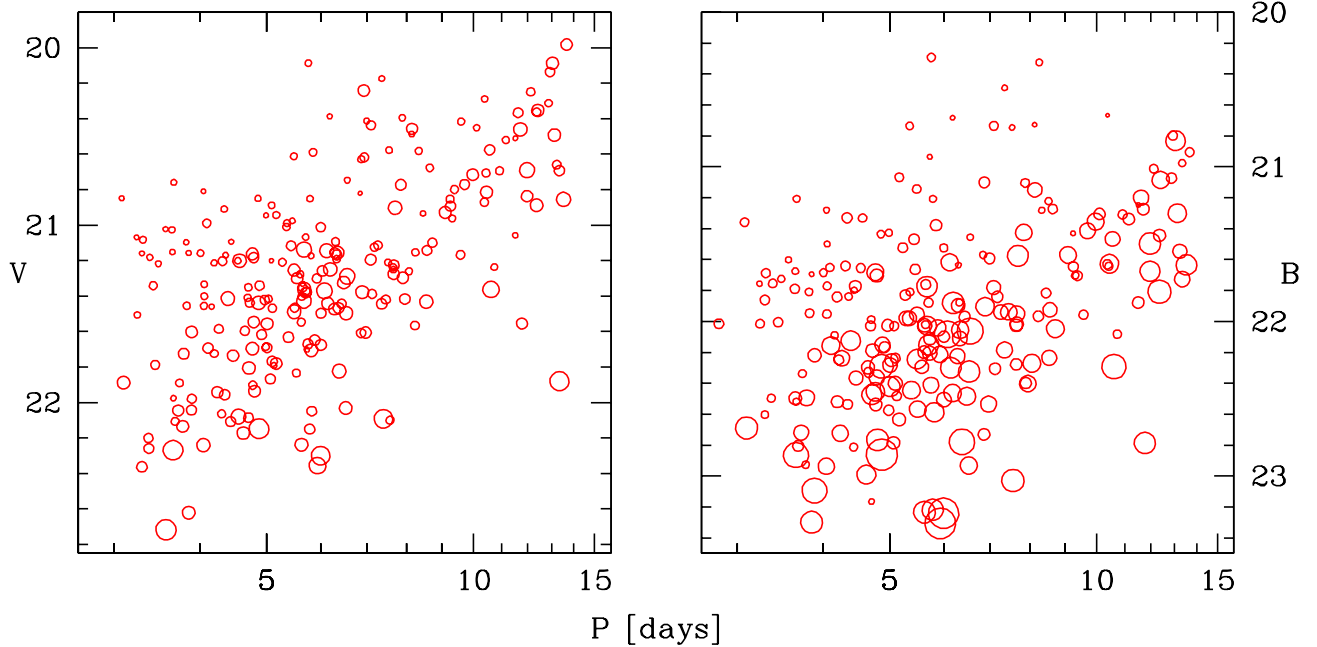


Fig. 11.— The V and B -band Period-Luminosity diagrams for the Cepheids in field M33A. The circles are proportional in size to their amplitudes in the corresponding band.

In Figure 11 we present the B and V -band P-L diagrams for the Cepheid variables, drawn as open circles proportional in size to their amplitudes. As expected, the amplitudes in the B -band are on average larger than in V . A clear relation between the period and magnitude is discernible. The several Cepheids too faint for their periods are probably suffering from greater than average reddening. Some of the faintest Cepheids exhibit quite large amplitudes. This is not a physical effect and is most likely caused by a similar phenomenon to the one discussed in Subsection 4.6 regarding the comparison with Paper VI photometry. If the magnitude used to convert the light curve from flux to magnitudes is measured too faint, the resulting amplitude will be too large.

For periods shorter than 8 days the relations widen upwards considerably, with the brighter Cepheids for a given period having smaller amplitudes. One possibility is that these Cepheids are pulsating in the first overtone. On the other hand these could be fundamental mode Cepheids which are heavily affected by blending: adding a constant flux would tend to increase the brightness of a Cepheid and diminish its amplitude. We will examine these stars in more depth in Section 6.

Figure 12 shows the location of the EBs and Cepheids within the field M33A. The Cepheids are plotted as open circles, proportional in size to their period and the EBs as open squares. To trace the spiral pattern of the galaxy we plot in the background all the stars with $V < 21.5$ mag as filled dots of size proportional to their magnitude. These two types of variables appear somewhat more plentiful within the spiral arms.

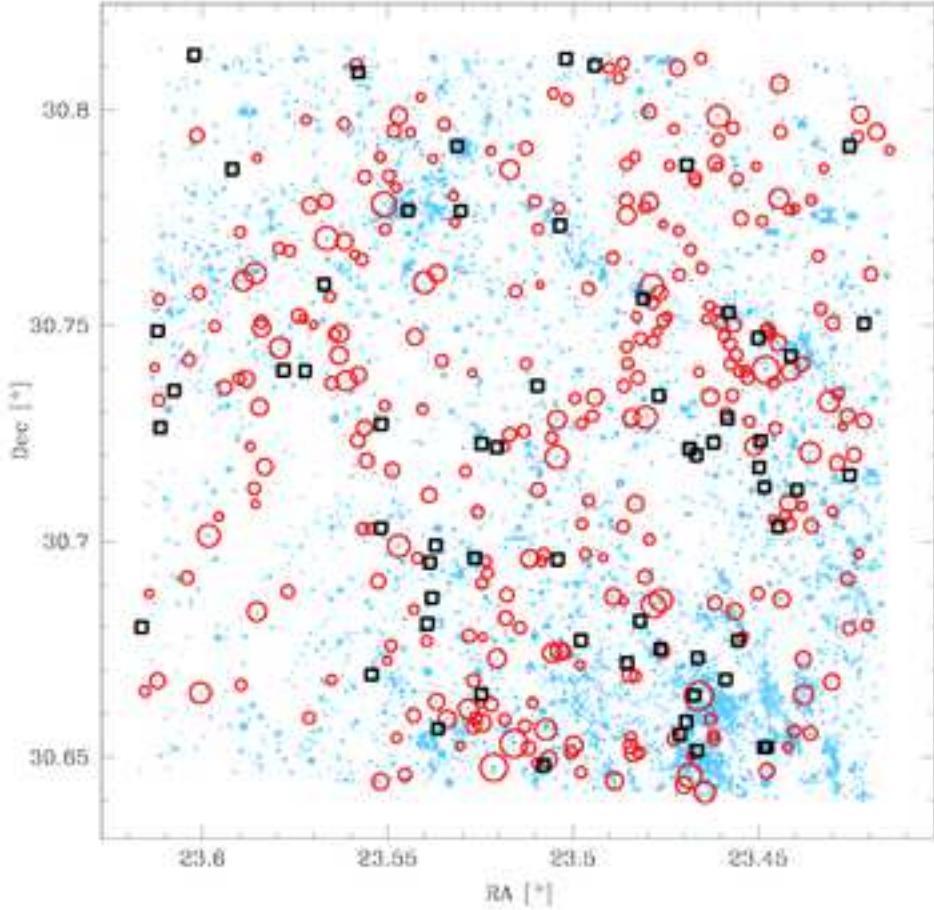


Fig. 12.— The location of EBs (squares) and Cepheids (circles) in the field of M33A. The size of the Cepheid symbols are proportional to their period. All other stars in the field with $V < 21.5$ mag are drawn as dots of size proportional to their magnitude.

6. First Overtone Cepheids

As we have noted in the previous Section, on the B and V -band P-L diagrams in Fig. 11 there are Cepheids which seem too bright for their periods. In addition they possess smaller pulsational amplitudes of variability compared to the normal Cepheids. Their positions on the P-L diagrams would lead us to expect that these should be first overtone (FO) pulsators (as in Fig. 2 of Udalski et al. 1999; hereafter U99). The situation is, however, complicated by the existence of blending. As a result of blending the Cepheid should appear brighter because of the added constant flux and its amplitude, measured in magnitudes, should decrease (Mochejska et al. 2000, 2001; Stanek & Udalski 1999).

In order to try to determine whether these Cepheids are first overtone pulsators, we have

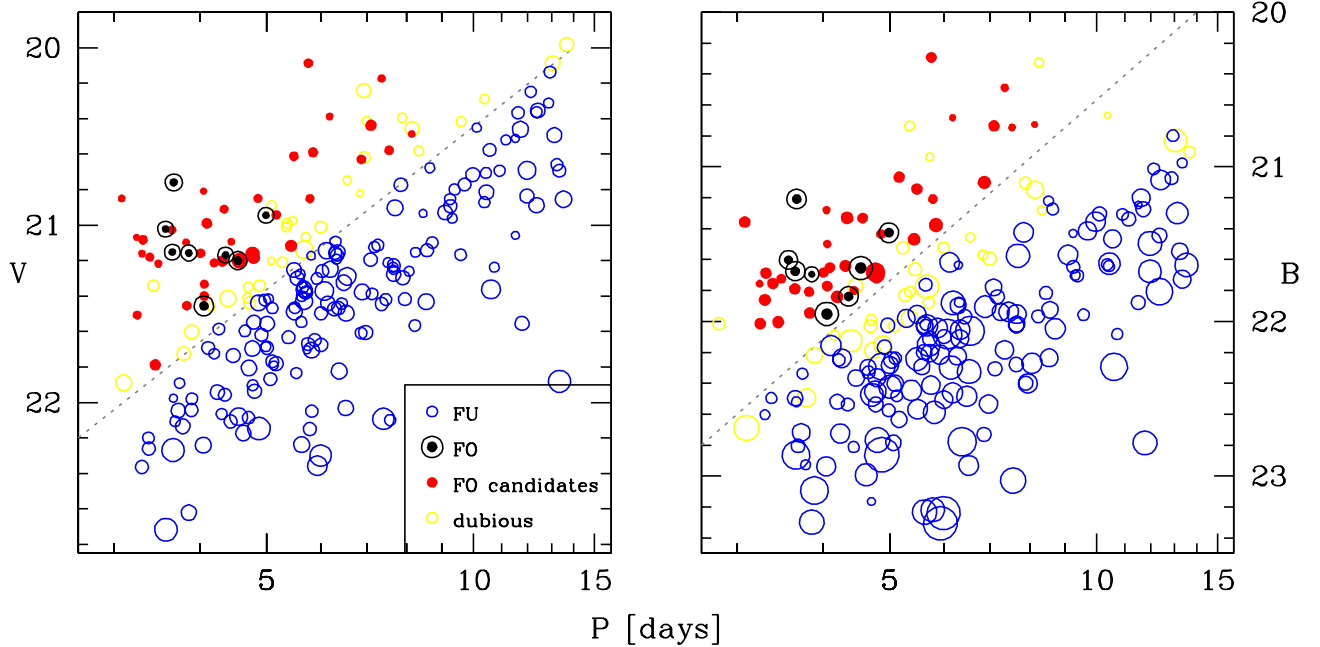


Fig. 13.— The V and B -band Period-Luminosity diagrams for the Cepheids in field M33A. The circles are proportional in size to the pulsational amplitudes of the Cepheids in the corresponding band. The dotted lines show the division between FU (open circles) and FO (filled circles) Cepheids. The encircled dots represent the most reliable FO Cepheid candidates. The light open circles show the Cepheids which are above the line in one band only.

checked whether they possess other properties expected of such stars. In addition to being brighter and having a smaller amplitude, Cepheids pulsating in the first overtone should have more symmetric (sinusoidal) light curves and be on average bluer than fundamental mode Cepheids (FU). The most powerful technique for discriminating them from FU Cepheids are the Fourier parameters of their light curves (Antonello & Aikawa 1995; Beaulieu et al. 1995).

To select a sample of FO Cepheid candidates we have made a division on the P-L diagrams roughly parallel to the P-L relation, between the bright low amplitude and fainter high amplitude Cepheids (dotted lines on Fig. 13). In our final sample we included the Cepheids which were above these lines in both of the P-L diagrams. There are 44 such Cepheids in our catalog (filled circles). FO Cepheids should have periods ranging from 1.7 to 6 days. We decided not to make a cutoff at higher periods, although we did not regard it likely that Cepheids with $P > 6$ days would turn out to be FO pulsators.

On the $V/B - V$ CMD (Fig. 14) we plot the positions of the FU Cepheids (open circles) and FO candidates (filled circles). As expected of FO Cepheids, our candidates are bluer than the FU ones. We note that on the CMD presented by U99 for the Large Magellanic Cloud (LMC) Cepheids (Fig. 4 therein) there is also some overlap between the loci of those two types of

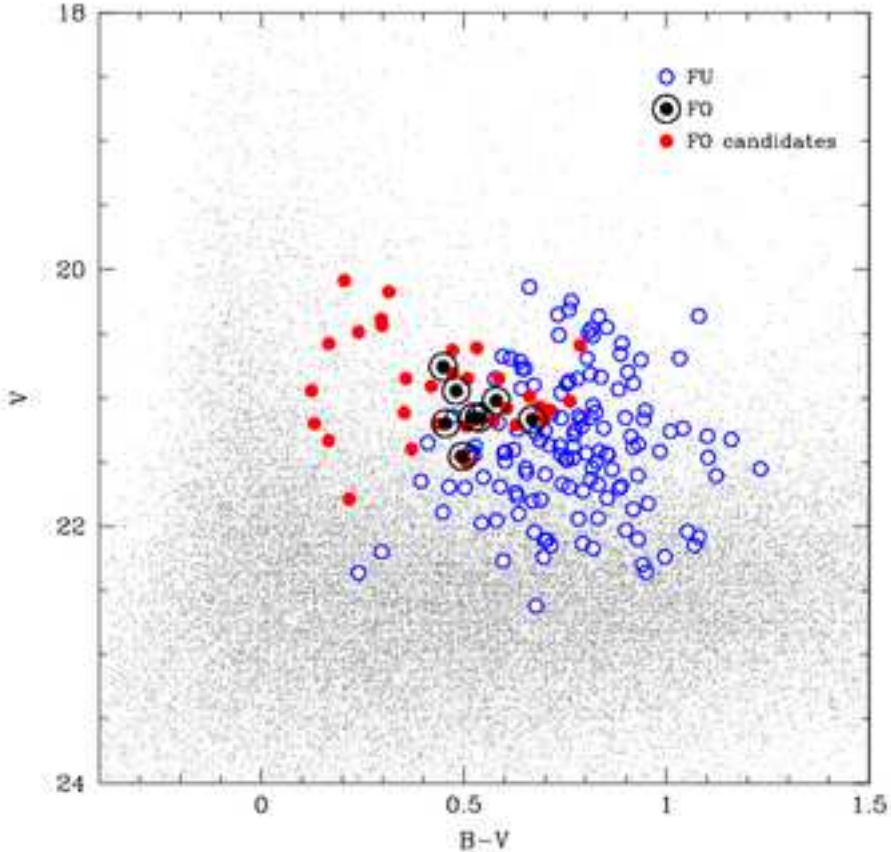


Fig. 14.— The $V/B - V$ CMD for the Cepheid variables. The FU Cepheids are denoted by open circles and the FO ones by filled circles. The encircled dots represent the most reliable FO Cepheid candidates.

Cepheids.

The relations between the light curve Fourier parameters $R_{21} = A_2/A_1$, $\phi_{21} = \phi_2 - 2\phi_1$ and the period for the FO Cepheid candidates (filled circles) and FU mode pulsators (open circles) are shown in Fig. 15. We have compared them with Fig. 3 in U99 for LMC Cepheids. We notice on the $R_{21}/\log P$ diagram for LMC that within our range of periods the FO Cepheids progress upwards in R_{21} with increasing period, forming the second branch of the V-shaped pattern and then merge with the FU Cepheid sequence at higher periods. The situation is very similar on the $\phi_{21}/\log P$ diagram in U99, where on the one hand the FU Cepheids are confined to a narrower sequence, but on the other there is more overlap between them and the FO pulsators.

Indeed we do observe in Fig. 15 the FO Cepheid candidates to occupy roughly the predicted positions despite our larger scatter in the Fourier parameters than in U99. From the $\phi_{21}/\log P$ diagram in the right panel we have selected eight FO Cepheids which are most separated from the FU Cepheid sequence. We examined their positions on the R_{21} diagram to find that they are

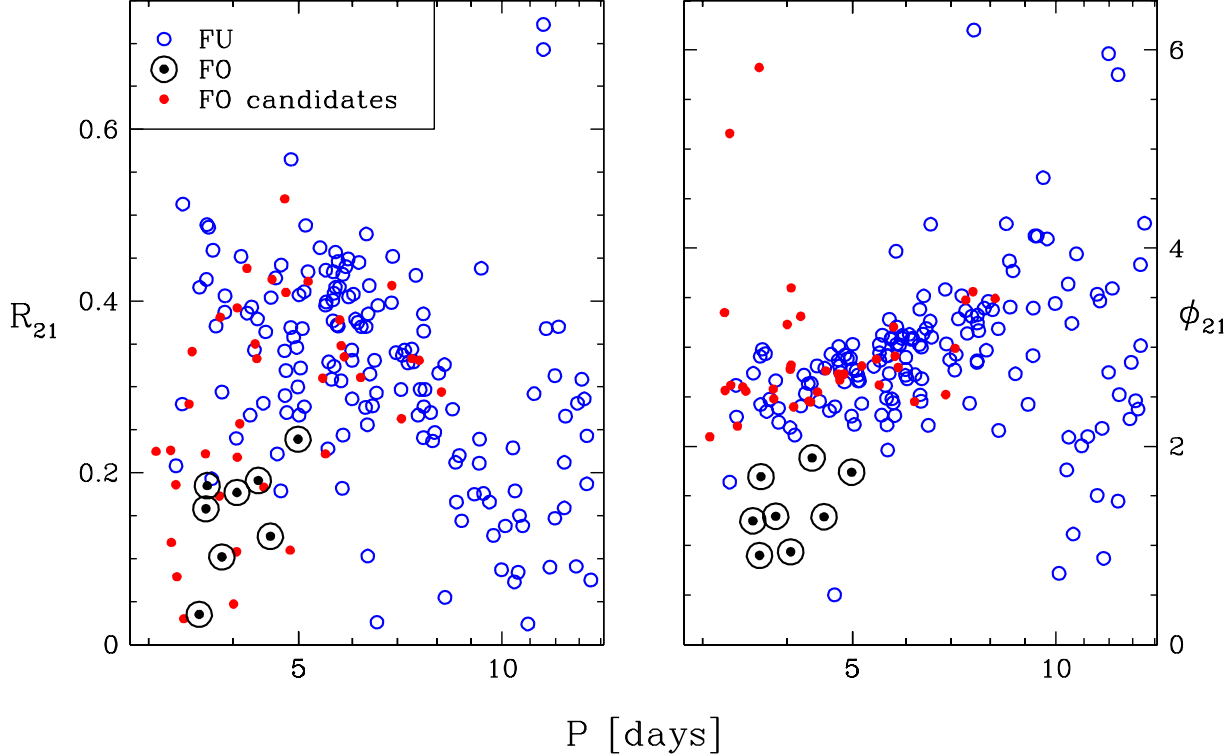


Fig. 15.— The Fourier parameters R_{21} and ϕ_{21} of the Cepheid light curves as a function of period. The FU Cepheids are denoted by open circles and the FO ones by filled circles. The encircled dots represent the most reliable FO Cepheid candidates.

also rather well separated from the FU mode Cepheids, especially the seven with shorter periods. These eight bona fide FO Cepheid candidates are denoted by encircled dots on Figs 13–15.

We have checked the brightest of these Cepheids, D33J013359.5+304017.0, which is unusually bright even for an overtone Cepheid, in archival HST data. It has two nearby companions, one of which appears bright enough to affect its photometry. To try to estimate the influence of blending on the Fourier parameters R_{21} and ϕ_{21} we have generated two new light curves for each of the eight best FO Cepheid candidates, one with an $S_V = \frac{f_{blend}}{f_{ceph}} = 0.5$ blend added and one with the same blend subtracted. The average differences between the original and recomputed parameters were 9% for R_{21} and 6% for ϕ_{21} . These differences are too small to change the positions of the Cepheids considerably on the R_{21} and ϕ_{21} diagrams. This very weak dependence of the Fourier parameters on blending strengthens our conclusion that these Cepheids are indeed first overtone pulsators.

As for the rest of the candidates, we believe many of them may also be FO Cepheids. More accurate photometry obtained with a larger instrument would be necessary to obtain better Fourier parameters of their light curves and resolve this issue.

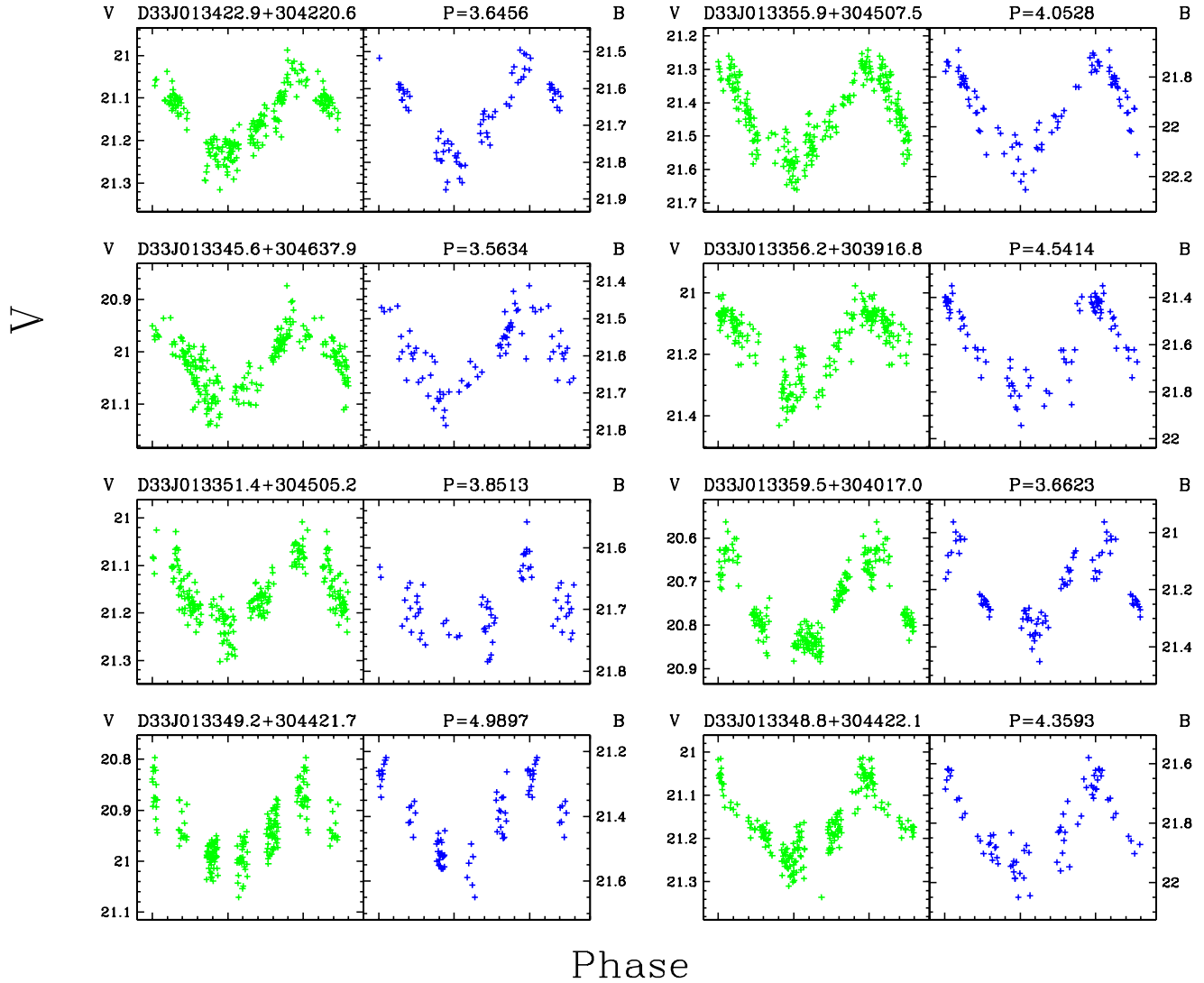


Fig. 16.— The V and B -band light curves of the eight FO Cepheids in the field M33A.

In Figure 16 we show the light curves of the eight FO Cepheids. They appear more symmetrical in shape and do not exhibit the fast rise and slow decline typical for FU Cepheids (see Fig. 6). This fact lends further credibility to the notion that these Cepheids pulsate in the first overtone.

7. Conclusions

Our search for variable stars in the data from the followup observations of the detached eclipsing binary D33J013346.2+304439.9 in field M33A collected at the 2.1m KPNO telescope resulted in the discovery of 63 eclipsing binaries, 305 Cepheids, and 66 other periodic, possible long period or non-periodic variables. Out of the total 434 variables 280 are not listed in our first M33

catalog (Paper VI). Due to the short time base of our observations, we were limited to variables with periods not exceeding 14 days. Thanks to the use of a larger aperture instrument and a novel method of image reduction – the ISIS image subtraction package, we were more efficient at finding the fainter and lower amplitude variables than in our previous study of this field, especially for short period Cepheids ($P < 8d$). We have also found a population of Cepheids which are most likely pulsating in the first overtone and for eight of them we present strong arguments in favor of this interpretation.

The method of image subtraction has two main advantages over the classical profile fitting method. It is more efficient in discovering variables: we have discovered 355 periodic variables using ISIS and only 212 with Dophot. Additionally in crowded fields image subtraction can lead to large improvements in the photometric accuracy (Alard 2000b).

During our first observing run we have found that the T2KA CCD camera produced a non-linear response to signal. We have obtained a set of calibration frames to determine a correction for the non-linearity to be applied to the science data. Although the comparison between images of differing exposure times (Fig. 3) and with the Macri et al. (2001b) stellar object catalog (Fig. 7) do not show marked non-linearity, some traces of it still remain. The presence of a residual non-linearity prevented us from obtaining an independent calibration. During the analysis of the data collected at KPNO in October 1998 with the T1KA camera we have found it to be also non-linear. We would like to caution the astronomical community of the problems we have encountered with the T1KA and T2KA cameras.

We thank the TAC of the KPNO for the generous allocation of the observing time. We would like to thank Lucas Macri for his help and for the analysis of T1KA non-linearity, Grzegorz Pojmański for *lc* - the light curve analysis utility and Wojtek Pych for his software. We thank the referee, Douglas Welch, for a prompt and useful report. BJM and JK were supported by the Polish KBN grant 2P03D003.17. BJM was also supported by the Polish KBN grant 2P03D025.19 and JK by the NSF grant AST-9819787. Support for KZS was provided by NASA through Hubble Fellowship grant HF-01124.01-A from the Space Telescope Science Institute, which is operated by the Association of Universities for Research in Astronomy, Inc., under NASA contract NAS5-26555. DDS acknowledges support from the Alfred P. Sloan Foundation and from NSF grant No. AST-9970812.

REFERENCES

- Alard, C., Lupton, R. 1998 *ApJ*, 503, 325
- Alard, C. 2000a *A&AS*, 144, 363
- Alard, C. 2000b *ASP Conf. Ser.* 203, *The Impact of Large-Scale Surveys on Pulsating Star Research*, ed. L. Szabados & D. Kurtz (San Francisco: ASP), 50

Andersen, J. 1991, A&AR, 3, 91

Antonello, E. & Aikawa, T. 1995, A&A, 302, 105

Beaulieu, J. P. et al. 1995, A&A, 303, 137

Freedman, W. L., Wilson, C. D., & Madore, B. F. 1991, ApJ, 372, 455

Guinan, E. F., et al. 1998, ApJ, 509, L21

Hilditch, R. W. 1996, in: ASP Conf. Ser. 90, The Origins, Evolution and Destinies of Binary Stars in Clusters, ed. E. F. Milone & J.-C. Mermilliod (San Francisco: ASP), 207

Holland, S. 1998, AJ, 115, 1916

Hubble, E. 1926, ApJ, 63, 236

Huterer, D., Sasselov, D. D., Schechter, P. L. 1995, AJ, 110, 2705

Kaluzny, J. & Udalski, A. 1992, Acta Astronomica, 42, 29

Kaluzny, J., Stanek, K. Z., Krockenberger, M., Sasselov, D. D., Tonry, J. L., & Mateo, M. 1998, AJ, 115, 1016 (Paper I)

Kaluzny, J., Mochejska, B. J., Stanek, K. Z., Krockenberger, M., Sasselov, D. D., Tonry, J. L., & Mateo, M. 1999, AJ, 118, 346 (Paper IV)

Kinman, T. D., Mould, J. R. & Wood, P. R. 1987, AJ, 93, 833

Krockenberger, M., Sasselov, D. D., & Noyes, R. 1997, ApJ, 479, 875

Landolt, A. 1992, AJ, 104, 340

Macri, L. M., Stanek, K. Z., Sasselov, D. D., Krockenberger, M., Kaluzny, J. 2001a, AJ, in press (Paper VI)

Macri, L. M., Stanek, K. Z., Sasselov, D. D., Krockenberger, M., Kaluzny, J. 2001b, AJ, in press

Mochejska, B. J., Kaluzny, J., Stanek, K. Z., Krockenberger, M. & Sasselov, D. D. 1999, AJ, 118, 2211 (Paper V)

Mochejska, B. J., Macri, L. M., Sasselov, D. D., & Stanek, K. Z. AJ, 2000, 120, 810

Mochejska, B. J., Macri, L. M., Sasselov, D. D., & Stanek, K. Z. 2001, in preparation

Monet, D., et al. 1996, USNO-SA2.0, (U.S. Naval Observatory, Washington DC).

Paczyński, B. 1997, in The Extragalactic Distance Scale, ed. M. Livio, M. Donahue & N. Panagia (Cambridge: Cambridge Univ. Press), 273

Schwarzenberg-Czerny, A. 1989, MNRAS, 253, 198

Stanek, K. Z., Kaluzny, J., Krockenberger, M., Sasselov, D. D., Tonry, J. L., & Mateo, M. 1998, AJ, 115, 1894 (Paper II)

Stanek, K. Z., Kaluzny, J., Krockenberger, M., Sasselov, D. D., Tonry, J. L., & Mateo, M. 1999, AJ, 117, 2810 (Paper III)

Stanek, K. Z., & Garnavich, P. M. 1998, *ApJ*, 503, L131

Stanek, K. Z. & Udalski, A. 1999, preprint (astro-ph/9909346)

Stetson, P. B. 1987, *PASP*, 99, 191

Udalski, A., Pietrzyński, G., Woźniak, P. R., Szymański, M., Kubiak, M., & Źebruń, K., 1998, *ApJ*, 509, L25

Udalski, A., Soszyński, I., Szymański, M., Kubiak, M., Pietrzyński, G., Woźniak, P. & Źebruń, K. 1999, *Acta Astronomica*, 49, 223 (U99)

Table 2. DIRECT ECLIPSING BINARIES IN M33A

Name	<i>P</i> (days)	<i>V_{max}</i>	<i>B_{max}</i>	<i>R₁</i>	<i>R₂</i>	<i>i</i> (deg)	<i>e</i>	Comments
D33J013413.0+304008.8	0.9574	20.90	20.98	0.58	0.37	51.94	0.03	
D33J013422.1+304710.4	1.0530	19.86	19.96	0.66	0.34	61.62	0.00	(1)
D33J013424.5+304845.8	1.0699	...	21.03	0.62	0.35	58.18	0.00	
D33J013400.4+304842.7	1.2517	21.24	21.26	0.39	0.26	71.20	0.01	
D33J013352.1+303951.4	1.2529	21.18	...	0.42	0.26	73.13	0.01	
D33J013347.6+303908.3	1.3211	20.23	...	0.39	0.29	59.22	0.00	
D33J013427.9+304048.3	1.3919	...	20.70	0.52	0.47	57.87	0.03	
D33J013426.9+304455.5	1.4173	20.87	20.90	0.48	0.28	62.79	0.01	
D33J013352.4+304317.2	1.4869	20.45	...	0.63	0.36	58.91	0.00	
D33J013352.5+304317.0	1.5229	20.45	...	0.56	0.38	58.74	0.00	
D33J013350.9+304322.6	1.5906	20.14	20.19	0.51	0.36	58.19	0.00	
D33J013409.4+304051.0	1.6053	20.93	...	0.46	0.33	65.80	0.01	
D33J013408.9+304156.6	1.6270	21.33	21.25	0.31	0.21	75.93	0.02	
D33J013425.8+304405.8	1.6818	20.67	20.73	0.43	0.40	53.71	0.00	
D33J013417.3+304422.4	1.7175	21.28	...	0.42	0.30	82.52	0.02	
D33J013407.5+304729.8	1.8102	19.11	19.15	0.62	0.35	34.34	0.03	
D33J013354.4+304401.7	1.8483	20.81	20.87	0.62	0.38	57.05	0.00	(1)
D33J013347.4+303908.0	1.8775	20.59	20.57	0.52	0.36	68.61	0.03	
D33J013413.9+304831.2	2.1098	20.89	20.72	0.54	0.44	84.89	0.01	
D33J013345.5+304242.7	2.1458	19.42	19.63	0.55	0.43	82.62	0.00	(1)
D33J013359.5+304037.6	2.1554	21.66	21.22	0.66	0.34	80.76	0.01	
D33J013347.9+304323.8	2.2497	21.31	...	0.48	0.31	54.45	0.09	
D33J013410.7+304635.8	2.3354	19.43	19.57	0.48	0.32	61.28	0.00	
D33J013347.6+304245.3	2.3616	21.40	21.33	0.25	0.15	77.85	0.08	
D33J013416.1+304534.4	2.3873	21.78	21.65	0.33	0.31	79.90	0.00	
D33J013352.6+304713.8	2.4157	20.69	20.73	0.57	0.38	52.68	0.00	
D33J013412.4+304211.1	2.5433	21.50	21.11	0.36	0.26	70.85	0.02	
D33J013405.9+303952.5	2.5678	20.55	20.60	0.56	0.37	65.58	0.00	
D33J013402.3+304409.6	2.6614	19.49	19.66	0.47	0.36	64.42	0.00	(1)
D33J013354.3+304029.6	2.7104	19.12	19.21	0.62	0.38	60.52	0.01	(1)
D33J013342.1+304255.3	2.7169	21.08	20.96	0.31	0.31	68.40	0.04	
D33J013412.4+304337.9	2.7724	...	20.25	0.68	0.32	60.43	0.02	(1)
D33J013355.6+304053.6	2.9579	20.29	20.25	0.41	0.24	66.10	0.02	
D33J013352.0+303905.0	2.9684	19.08	19.23	0.70	0.30	68.64	0.02	(1)
D33J013401.0+304144.9	3.3907	19.78	20.05	0.46	0.34	60.38	0.00	
D33J013352.0+304312.4	3.4623	20.23	20.21	0.50	0.50	56.63	0.00	(1)
D33J013409.3+304142.1	3.5901	20.59	20.59	0.64	0.36	47.33	0.00	
D33J013400.8+304623.5	3.7015	21.17	21.26	0.63	0.37	64.12	0.01	
D33J013418.8+304422.7	3.8052	21.12	21.24	0.44	0.32	77.96	0.01	
D33J013356.5+304018.4	3.8364	20.11	20.28	0.57	0.34	68.13	0.01	(1)

Table 2. CONTINUED

Name	P (days)	V_{max}	B_{max}	R_1	R_2	i (deg)	e	Comments
D33J013349.3+304037.1	3.8427	19.54	...	0.49	0.32	65.81	0.00	(1)
D33J013405.9+304321.4	4.1309	19.60	19.79	0.47	0.24	57.59	0.01	
D33J013407.3+304635.5	4.4172	19.61	19.77	0.59	0.40	61.07	0.01	(1)
D33J013347.9+304301.6	4.4363	19.63	19.75	0.46	0.36	71.74	0.01	(1)
D33J013350.0+304342.8	4.4808	20.60	20.71	0.34	0.21	89.87	0.01	
D33J013409.1+304112.7	4.7310	20.72	20.92	0.31	0.25	74.58	0.10	
D33J013353.1+303919.1	4.7424	19.77	19.45	0.63	0.37	69.68	0.00	
D33J013426.7+304334.8	6.2106	...	19.81	0.59	0.41	53.11	0.03	(1)
D33J013341.1+304501.7	6.8336	19.60	19.57	0.57	0.43	70.95	0.03	(1)
D33J013346.7+304212.3	6.9221	19.55	19.58	0.48	0.41	65.75	0.06	(1)
D33J013348.0+304449.6	7.2528	18.97	18.95	0.61	0.38	42.51	0.00	(1)
D33J013404.9+304318.4	7.2917	20.22	20.18	0.69	0.30	89.87	0.00	(1)
D33J013342.1+304729.7	22.9536	18.53	18.36	0.53	0.46	57.77	0.13	(1)

Note. — (1) Variables identified by Macri et al. (2001a)

Table 3. DIRECT FLUX
ECLIPSING BINARIES IN M33A

Name	P (days)
D33J013358.6+304837.0	1.1098
D33J013351.9+304022.7	1.3107
D33J013349.9+304510.7	2.1464
D33J013345.9+304434.7	2.3016
D33J013352.7+303929.4	2.4432
D33J013401.9+303852.9	2.6338
D33J013406.3+304145.9	3.0542
D33J013355.4+304522.5	3.3443
D33J013350.1+304004.6	3.3573
D33J013408.7+303923.6	4.3455

Table 4. DIRECT CEPHEIDS IN M33A

Name	P (days)	$\langle V \rangle$	$\langle B \rangle$	A_V	B_V	Comments
D33J013402.1+304534.0	2.823	...	22.02	...	0.22	
D33J013342.5+304335.4	3.077	20.85	21.36	0.07	0.19	
D33J013416.8+304500.5	3.097	21.89	22.69	0.33	0.63	
D33J013407.3+303909.7	3.234	21.07	21.76	0.06	0.09	
D33J013420.6+304231.3	3.241	21.51	22.01	0.12	0.19	
D33J013358.0+304146.4	3.292	21.16	21.86	0.07	0.22	
D33J013350.6+304712.9	3.293	22.36	22.60	0.25	0.15	
D33J013405.8+304040.2	3.304	21.08	21.69	0.13	0.20	
D33J013427.1+304425.0	3.364	22.20	22.50	0.21	0.17	
D33J013409.9+304810.6	3.371	22.26	...	0.23	...	
D33J013406.5+304420.5	3.381	21.18	21.75	0.11	0.19	
D33J013354.2+304624.3	3.421	21.34	...	0.17	...	
D33J013420.4+304719.9	3.443	21.79	22.00	0.20	0.22	
D33J013412.0+304020.2	3.478	21.22	21.72	0.10	0.14	
D33J013345.6+304637.9	3.563	21.02	21.60	0.07	0.11	
D33J013409.1+304719.0	3.569	22.72	...	0.57	...	
D33J013356.7+304110.5	3.641	21.03	21.79	0.11	0.21	
D33J013427.4+304116.6	3.645	...	22.50	...	0.32	
D33J013422.9+304220.6	3.646	21.15	21.68	0.09	0.13	
D33J013417.3+304505.3	3.654	22.27	22.86	0.55	0.72	(1)
D33J013343.8+304711.2	3.659	21.98	22.52	0.09	0.14	
D33J013359.5+304017.0	3.662	20.76	21.21	0.10	0.14	
D33J013347.0+304217.9	3.680	22.11	22.80	0.16	0.26	
D33J013420.9+304319.4	3.719	22.05	22.72	0.27	0.40	
D33J013354.5+304454.9	3.735	21.89	22.34	0.16	0.17	
D33J013339.5+304726.4	3.775	22.13	22.93	0.30	0.15	
D33J013407.7+304648.4	3.788	21.73	22.49	0.26	0.42	
D33J013410.5+304741.2	3.818	21.10	21.81	0.08	0.16	
D33J013348.1+304712.8	3.826	21.45	21.95	0.14	0.19	
D33J013351.4+304505.2	3.851	21.16	21.70	0.08	0.06	
D33J013414.1+304559.1	3.852	22.62	23.30	0.32	0.62	
D33J013353.9+304507.5	3.888	22.04	23.09	0.24	0.72	
D33J013417.3+304751.5	3.890	21.60	22.22	0.29	0.34	
D33J013405.3+304725.8	3.892	21.98	...	0.20	...	
D33J013404.4+304319.4	4.006	21.16	21.68	0.13	0.16	
D33J013410.3+304103.3	4.045	22.24	22.94	0.34	0.44	
D33J013406.0+303945.0	4.048	20.81	21.28	0.06	0.10	
D33J013355.9+304507.5	4.053	21.45	21.95	0.14	0.19	
D33J013407.6+304626.5	4.057	21.33	21.50	0.12	0.10	
D33J013411.4+304655.3	4.058	21.40	21.77	0.13	0.17	

Table 4. CONTINUED

Name	P (days)	$\langle V \rangle$	$\langle B \rangle$	A_V	B_V	Comments
D33J013351.8+304421.3	4.093	20.99	21.65	0.18	0.18	
D33J013413.1+304210.5	4.110	21.69	22.16	0.25	0.49	(1)
D33J013350.7+304512.1	4.158	21.46	22.09	0.07	0.15	
D33J013402.3+303855.0	4.193	21.21	21.84	0.11	0.23	
D33J013415.6+304004.4	4.197	21.73	22.52	0.16	0.30	
D33J013345.1+304229.4	4.219	...	22.25	...	0.22	
D33J013353.7+304713.5	4.240	21.94	22.72	0.28	0.44	
D33J013412.5+304720.7	4.261	21.59	22.24	0.20	0.42	
D33J013411.4+303916.2	4.301	22.06	23.75	0.17	0.68	
D33J013353.5+304744.1	4.312	21.20	21.64	0.19	0.22	
D33J013343.2+304224.9	4.337	20.91	21.33	0.12	0.24	
D33J013346.0+304637.0	4.346	21.96	22.54	0.25	0.23	
D33J013348.8+304422.1	4.359	21.17	21.84	0.09	0.15	
D33J013351.9+304658.7	4.391	21.41	22.12	0.35	0.54	(1)
D33J013427.7+303954.9	4.434	22.11	22.81	0.24	0.17	
D33J013349.0+304040.4	4.441	21.09	21.80	0.08	0.12	
D33J013402.6+303944.5	4.459	...	21.77	...	0.30	(1)
D33J013412.2+304353.1	4.470	21.74	22.36	0.28	0.36	(1)
D33J013356.2+303916.8	4.541	21.20	21.66	0.12	0.20	
D33J013356.0+304720.8	4.551	22.08	...	0.39	...	
D33J013350.9+303918.3	4.568	21.20	21.33	0.35	0.18	
D33J013401.2+304813.7	4.624	22.17	22.99	0.32	0.53	
D33J013415.7+304524.3	4.650	21.60	22.30	0.21	0.33	
D33J013351.7+304548.1	4.661	...	22.33	...	0.23	
D33J013409.4+304036.8	4.694	21.41	22.03	0.15	0.23	
D33J013355.0+304201.6	4.702	21.35	21.99	0.15	0.16	
D33J013341.0+304049.6	4.707	22.09	23.16	0.22	0.09	
D33J013402.0+304143.5	4.713	21.80	22.48	0.32	0.56	
D33J013407.0+304258.5	4.725	21.44	22.19	0.21	0.35	
D33J013421.6+304618.2	4.767	21.70	22.45	0.32	0.52	(1)
D33J013409.7+304350.4	4.768	21.16	21.68	0.30	0.45	(1)
D33J013402.2+304620.8	4.774	21.90	22.54	0.18	0.31	
D33J013351.1+304516.0	4.790	21.18	21.70	0.24	0.34	
D33J013359.4+304214.2	4.790	21.55	22.36	0.28	0.40	(1)
D33J013423.2+304459.3	4.803	21.94	22.77	0.29	0.62	
D33J013347.8+304627.4	4.858	20.85	21.43	0.11	0.15	
D33J013426.8+304522.0	4.869	21.44	22.29	0.35	0.68	(1)
D33J013403.0+304428.1	4.874	22.15	22.86	0.55	0.93	
D33J013412.2+304620.4	4.883	21.34	22.15	0.21	0.41	
D33J013419.0+304604.6	4.916	21.62	22.17	0.23	0.27	

Table 4. CONTINUED

Name	P (days)	$\langle V \rangle$	$\langle B \rangle$	A_V	B_V	Comments
D33J013359.9+304359.3	4.969	21.42	22.02	0.21	0.29	
D33J013400.9+304637.9	4.987	21.68	22.57	0.14	0.24	
D33J013349.2+304421.7	4.990	20.95	21.43	0.07	0.14	
D33J013357.0+304826.4	5.008	21.69	22.28	0.23	0.38	(1)
D33J013359.4+304338.4	5.008	21.56	22.42	0.30	0.56	
D33J013421.5+304000.2	5.033	21.41	22.25	0.15	0.34	(1)
D33J013352.4+304603.3	5.065	21.87	22.79	0.24	0.32	
D33J013405.9+304124.9	5.081	21.20	22.03	0.05	0.20	
D33J013351.7+304843.1	5.087	20.89	...	0.12	...	
D33J013418.3+304602.4	5.097	21.77	22.40	0.24	0.37	
D33J013400.4+304808.8	5.099	21.47	22.24	0.18	0.22	(1)
D33J013410.1+304146.0	5.123	21.79	22.48	0.10	0.21	
D33J013341.5+304737.7	5.164	21.78	22.63	0.28	0.33	(1)
D33J013348.6+304340.0	5.164	20.94	21.07	0.14	0.19	
D33J013359.2+304149.4	5.228	...	21.52	...	0.22	
D33J013350.2+304451.1	5.271	21.21	21.83	0.16	0.25	
D33J013359.0+304233.8	5.291	...	21.98	...	0.39	
D33J013421.6+304415.9	5.344	21.01	21.98	0.15	0.37	(1)
D33J013347.5+304456.2	5.348	...	20.73	...	0.15	
D33J013347.2+304452.5	5.355	20.99	21.81	0.14	0.16	
D33J013405.5+304133.3	5.380	21.63	22.45	0.25	0.48	(1)
D33J013358.7+304344.8	5.428	21.12	21.47	0.22	0.25	
D33J013359.5+303846.8	5.450	20.98	21.66	0.10	0.24	(1)
D33J013415.4+304452.8	5.479	20.61	21.14	0.13	0.19	(1)
D33J013355.3+304638.6	5.482	21.25	21.95	0.30	0.39	(1)
D33J013356.5+304442.4	5.484	21.49	22.24	0.35	0.55	
D33J013411.8+304033.0	5.494	21.46	22.57	0.20	0.45	
D33J013404.4+303931.3	5.524	21.83	...	0.17	...	
D33J013356.0+304007.5	5.540	21.30	...	0.28	...	
D33J013350.0+304346.7	5.572	...	22.29	...	0.35	(1)
D33J013347.0+304412.3	5.597	21.28	...	0.14	...	
D33J013346.2+304221.2	5.617	21.55	22.20	0.17	0.32	
D33J013402.5+304643.6	5.623	22.24	23.23	0.33	0.62	
D33J013356.5+304714.7	5.626	21.40	22.02	0.16	0.36	
D33J013413.7+304555.0	5.641	21.33	22.02	0.07	0.17	
D33J013414.8+304748.4	5.644	21.35	21.76	0.19	0.23	
D33J013414.0+304837.7	5.669	21.43	22.03	0.38	0.52	(1)
D33J013401.3+304325.6	5.670	21.14	21.77	0.40	0.58	(1)
D33J013356.5+304428.2	5.671	21.36	...	0.34	...	
D33J013354.8+304447.0	5.700	21.07	21.88	0.12	0.21	

Table 4. CONTINUED

Name	P (days)	$\langle V \rangle$	$\langle B \rangle$	A_V	B_V	Comments
D33J013420.6+304244.2	5.700	21.38	22.15	0.25	0.56	(1)
D33J013342.8+304403.1	5.721	...	20.93	...	0.07	
D33J013403.4+304047.9	5.722	21.70	22.20	0.08	0.38	
D33J013406.2+304224.6	5.722	21.38	22.11	0.21	0.31	
D33J013350.6+304734.9	5.745	21.67	22.41	0.23	0.42	(1)
D33J013426.8+304357.7	5.752	20.09	20.29	0.13	0.18	(1)
D33J013353.1+304542.3	5.779	22.15	23.22	0.24	0.60	
D33J013354.8+304518.8	5.782	20.85	21.21	0.12	0.14	
D33J013355.7+303903.6	5.803	21.17	...	0.10	...	
D33J013408.3+304748.0	5.811	21.70	22.59	0.33	0.54	
D33J013357.4+304556.6	5.817	22.05	...	0.22	...	
D33J013420.2+304503.2	5.844	20.59	21.38	0.16	0.28	
D33J013349.8+304427.9	5.875	21.65	22.04	0.25	0.45	(1)
D33J013424.9+304431.2	5.921	21.30	22.21	0.21	0.44	(1)
D33J013411.9+304704.6	5.930	22.36	23.31	0.45	0.91	
D33J013355.6+304449.1	5.993	22.30	23.24	0.51	0.90	
D33J013346.9+304334.2	5.997	21.01	21.52	0.21	0.17	(1)
D33J013349.6+304744.7	6.000	21.67	22.51	0.26	0.39	(1)
D33J013408.5+304430.6	6.000	21.50	22.10	0.23	0.28	(1)
D33J013403.2+304332.0	6.027	21.26	...	0.25	...	(1)
D33J013359.0+304531.0	6.070	21.37	22.08	0.42	0.78	(1)
D33J013356.7+304838.6	6.116	21.14	21.62	0.37	0.47	(1)
D33J013356.7+304409.5	6.140	21.44	22.30	0.31	0.58	
D33J013342.1+304047.3	6.178	...	22.46	...	0.48	
D33J013406.3+303932.6	6.178	20.39	20.68	0.08	0.06	
D33J013403.7+304528.6	6.190	21.25	21.88	0.35	0.61	(1)
D33J013349.7+304401.6	6.280	21.47	22.22	0.29	0.40	
D33J013400.1+303904.2	6.292	21.16	21.90	0.24	0.35	
D33J013348.0+304116.8	6.298	21.09	21.64	0.17	0.09	
D33J013346.6+304741.7	6.319	21.19	21.88	0.15	0.14	
D33J013356.8+304212.2	6.329	21.17	22.11	0.23	0.39	
D33J013349.4+304701.9	6.335	21.16	22.05	0.35	0.47	(1)
D33J013401.9+304148.9	6.361	21.47	...	0.26	...	
D33J013403.1+303925.9	6.376	21.82	22.78	0.35	0.74	
D33J013424.2+304527.5	6.432	21.44	21.97	0.21	0.27	
D33J013410.9+303845.1	6.478	21.32	22.48	0.32	0.49	
D33J013349.8+304444.7	6.519	22.03	22.93	0.32	0.47	
D33J013415.6+304411.9	6.529	21.50	22.32	0.34	0.61	
D33J013425.0+304129.7	6.550	21.29	22.06	0.41	0.76	(1)
D33J013418.5+304118.1	6.553	20.75	21.46	0.10	0.12	

Table 4. CONTINUED

Name	P (days)	$\langle V \rangle$	$\langle B \rangle$	A_V	B_V	Comments
D33J013349.4+304435.5	6.842	20.82	21.57	0.04	0.14	
D33J013354.1+304028.1	6.862	21.61	22.73	0.21	0.29	
D33J013352.1+304702.9	6.870	20.63	21.10	0.14	0.26	(1)
D33J013355.8+304416.5	6.890	21.38	21.90	0.33	0.51	(1)
D33J013353.5+303915.3	6.926	20.24	...	0.29	...	
D33J013406.4+304003.7	6.937	20.62	...	0.20	...	(1)
D33J013413.5+304704.1	6.970	21.61	22.53	0.27	0.43	
D33J013411.6+304742.5	6.992	20.41	21.59	0.10	0.26	
D33J013403.0+304727.9	7.087	21.19	21.78	0.26	0.36	(1)
D33J013404.1+304329.3	7.095	20.44	20.73	0.20	0.20	(1)
D33J013410.3+303934.8	7.121	21.39	22.30	0.20	0.28	(1)
D33J013354.1+304504.0	7.177	21.12	21.84	0.17	0.28	
D33J013356.5+304644.6	7.260	21.11	21.94	0.19	0.38	
D33J013340.7+304543.1	7.355	21.44	22.18	0.25	0.43	
D33J013343.2+304502.1	7.356	20.17	20.49	0.10	0.10	
D33J013348.6+304416.8	7.397	22.09	...	0.51	...	
D33J013404.3+304115.4	7.455	21.42	21.94	0.20	0.45	
D33J013406.4+303925.6	7.510	21.21	...	0.13	...	
D33J013347.3+304456.5	7.540	20.58	20.75	0.13	0.09	
D33J013405.3+303943.8	7.565	22.10	23.03	0.17	0.64	
D33J013402.9+303907.6	7.646	21.24	22.28	0.14	0.28	
D33J013349.1+304629.4	7.647	21.25	22.02	0.12	0.32	
D33J013350.8+304108.6	7.656	21.28	21.95	0.27	0.44	
D33J013422.5+304408.4	7.660	21.23	22.02	0.25	0.35	(1)
D33J013424.4+304739.0	7.690	20.90	21.57	0.35	0.59	(1)
D33J013402.3+304242.9	7.840	20.77	21.42	0.26	0.45	(1)
D33J013344.6+304212.9	7.880	20.39	21.10	0.12	0.19	(1)
D33J013346.0+304214.6	7.894	21.30	22.40	0.28	0.27	
D33J013413.9+304324.3	7.950	21.42	22.40	0.25	0.44	(1)
D33J013341.8+304312.2	8.060	21.26	22.27	0.14	0.49	(1)
D33J013355.3+304130.4	8.134	20.49	20.73	0.09	0.06	
D33J013417.7+304508.1	8.140	20.46	21.15	0.27	0.38	(1)
D33J013404.3+304056.0	8.220	21.57	...	0.19	...	
D33J013412.6+304126.7	8.233	21.15	21.97	0.15	0.25	(1)
D33J013400.6+304027.8	8.257	...	20.32	...	0.12	
D33J013356.3+304008.6	8.328	20.58	21.28	0.14	0.11	
D33J013342.2+304344.5	8.447	20.93	21.82	0.09	0.23	
D33J013411.7+304259.5	8.523	...	21.22	...	0.14	
D33J013413.3+304307.3	8.539	21.43	22.23	0.34	0.40	(1)
D33J013416.0+304644.0	8.560	21.14	21.93	0.23	0.37	(1)

Table 4. CONTINUED

Name	P (days)	$\langle V \rangle$	$\langle B \rangle$	A_V	B_V	Comments
D33J013356.2+303909.1	8.640	20.68	21.27	0.15	0.21	(1)
D33J013409.3+304238.6	8.714	21.10	22.05	0.21	0.49	(1)
D33J013413.5+304334.7	9.098	20.93	21.57	0.30	0.46	(1)
D33J013342.9+304305.5	9.251	20.85	21.43	0.17	0.07	
D33J013426.9+304003.6	9.260	20.89	21.65	0.24	0.23	(1)
D33J013341.1+304340.7	9.316	20.96	21.70	0.13	0.15	
D33J013345.1+304021.8	9.388	20.80	21.70	0.17	0.22	
D33J013349.6+304501.0	9.582	21.17	21.96	0.19	0.21	
D33J013353.2+304835.2	9.600	20.42	...	0.14	...	(1)
D33J013350.8+304715.5	9.710	20.77	21.41	0.23	0.42	(1)
D33J013421.1+304415.5	9.980	20.72	21.36	0.29	0.46	(1)
D33J013408.8+303946.5	10.110	20.45	21.30	0.11	0.28	(1)
D33J013343.2+304002.7	10.376	20.87	21.63	0.18	0.21	
D33J013346.7+304445.6	10.383	20.29	20.67	0.12	0.03	
D33J013356.1+303903.0	10.430	20.71	21.64	0.17	0.17	(1)
D33J013410.2+304450.6	10.450	20.81	21.63	0.30	0.52	(1)
D33J013417.0+304640.2	10.560	20.58	21.47	0.24	0.40	(1)
D33J013413.9+304418.7	10.610	21.36	22.29	0.44	0.70	(1)
D33J013420.0+304302.3	10.727	21.24	22.08	0.13	0.18	
D33J013349.5+304101.5	10.919	20.69	21.31	0.17	0.20	
D33J013358.6+304400.1	11.150	20.52	21.34	0.14	0.29	(1)
D33J013340.3+304741.7	11.510	21.06	21.88	0.09	0.29	(1)
D33J013346.5+304111.8	11.511	20.51	21.25	0.07	0.05	
D33J013357.4+304113.9	11.620	20.37	21.20	0.22	0.41	(1)
D33J013401.6+303858.2	11.707	20.46	21.27	0.35	0.30	
D33J013414.7+304609.7	11.770	21.55	22.79	0.27	0.60	(1)
D33J013356.2+304343.0	11.970	20.84	21.68	0.28	0.56	(1)
D33J013420.3+304351.9	11.970	20.69	21.50	0.40	0.61	(1)
D33J013341.4+304756.1	12.120	20.25	21.01	0.18	0.19	(1)
D33J013346.6+304821.8	12.360	20.36	21.44	0.18	0.31	(1)
D33J013351.1+304400.4	12.360	20.89	21.81	0.32	0.67	(1)
D33J013411.3+304755.1	12.410	20.35	21.09	0.30	0.47	(1)
D33J013355.0+304643.2	12.870	20.31	21.07	0.15	0.24	(1)
D33J013346.0+304231.9	12.930	20.14	20.80	0.21	0.21	(1)
D33J013402.8+304145.7	13.040	20.09	20.83	0.30	0.55	(1)
D33J013345.9+304421.4	13.120	20.49	21.30	0.31	0.51	(1)
D33J013359.9+303910.3	13.230	20.66	21.55	0.19	0.37	(1)
D33J013357.3+303840.1	13.337	...	20.98	...	0.14	
D33J013415.1+304435.2	13.340	20.69	21.73	0.24	0.41	(1)
D33J013356.5+304632.1	13.348	21.88	...	0.54	...	(1) Type II

Table 4. CONTINUED

Name	<i>P</i> (days)	$\langle V \rangle$	$\langle B \rangle$	A_V	B_V	Comments
D33J013408.8+304543.5	13.530	20.85	21.63	0.37	0.58	(1)
D33J013400.9+304028.5	13.672	19.98	20.91	0.28	0.20	

Note. — (1) Variables identified by Macri et al. (2001a)

Table 5. DIRECT FLUX CEPHEIDS IN M33A

Name	<i>P</i> (days)	Comments
D33J013341.5+304149.7	3.400	
D33J013352.3+303901.0	3.663	
D33J013346.0+303908.3	4.087	
D33J013353.1+304619.1	4.426	
D33J013344.5+304644.8	4.536	
D33J013405.6+304143.5	4.716	
D33J013357.7+304834.8	4.856	
D33J013350.9+303914.6	5.362	
D33J013351.1+303931.4	5.457	
D33J013344.1+304558.1	5.568	(1)
D33J013417.1+303932.9	5.650	(1)
D33J013413.6+304210.5	5.867	(1)
D33J013343.9+304513.7	5.910	(1)
D33J013345.6+303921.5	6.008	
D33J013342.2+304128.3	6.559	
D33J013350.5+304502.0	6.763	
D33J013406.7+304041.2	6.766	
D33J013344.6+303919.9	7.452	
D33J013345.2+304428.2	7.599	
D33J013355.1+304758.5	8.242	
D33J013354.4+304527.2	8.747	
D33J013347.4+303848.5	9.066	
D33J013352.8+303836.6	11.168	
D33J013412.5+303839.8	11.240	(1)
D33J013356.0+304231.3	11.340	(1)
D33J013420.2+304457.9	12.934	
D33J013408.1+303931.9	13.320	(1)

Note. — (1) Variables identified by Macri et al. (2001a)

Table 6. DIRECT PERIODIC VARIABLES IN M33A

Name	P (days)	V^a	B^a	A_V	B_V	Comments
D33J013407.1+303925.6	1.58	19.51	19.30	0.01	0.02	
D33J013345.0+304449.3	1.65	18.76	...	0.03	...	EB
D33J013418.4+304552.2	1.97	...	21.55	...	0.68	EB
D33J013426.4+304033.3	2.24	20.70	...	0.05	...	EB
D33J013340.9+303911.0	2.45	21.13	21.38	0.28	0.32	EB
D33J013345.9+304748.6	2.51	21.40	21.30	0.11	0.41	EB
D33J013427.3+304311.6	3.59	...	21.87	...	0.53	EB
D33J013349.3+303835.2	4.99	19.20	19.53	0.04	0.01	
D33J013344.2+304214.7	6.11	20.10	20.20	0.31	0.19	EB
D33J013352.4+303840.2	6.38	19.90	19.75	0.06	0.03	
D33J013346.0+304658.5	6.46	21.21	21.72	0.27	0.57	EB
D33J013409.2+304641.4	11.65	18.31	18.31	0.02	0.03	
D33J013405.5+304726.3	13.17	18.33	18.50	0.02	0.02	

Note. — ^a The V and B columns list the maximum magnitudes V_{max} and B_{max} for the eclipsing variables and flux-weighted average magnitudes $\langle V \rangle$ and $\langle B \rangle$ for the other variables.

Table 7. DIRECT MISCELLANEOUS VARIABLES IN M33A

Name	\bar{V}	\bar{B}	A_V	B_V	Comments
D33J013339.7+304541.6	17.27	17.25	0.46	0.20	
D33J013407.5+304721.4	19.24	...	0.13	...	
D33J013412.7+304728.2	19.37	...	0.23	...	
D33J013416.8+304518.8	19.37	21.26	0.61	0.52	(1)
D33J013344.8+304249.9	19.41	20.51	0.14	0.13	
D33J013416.6+304750.9	19.55	...	0.22	...	(1)
D33J013348.8+304212.0	19.62	...	0.20	...	(1)
D33J013345.8+304438.1	19.81	...	0.17	...	
D33J013347.5+304630.9	19.94	21.70	0.28	0.37	(1)
D33J013350.5+303836.3	19.98	...	0.96	...	
D33J013409.4+304527.3	20.00	21.62	0.24	0.34	(1)
D33J013421.0+304743.0	20.18	21.67	0.30	0.53	
D33J013342.3+304024.7	20.27	20.26	0.11	0.07	
D33J013420.1+304436.9	20.40	22.07	0.39	0.47	(1)
D33J013409.7+304100.2	20.49	21.91	0.52	0.64	
D33J013345.9+304312.4	20.50	20.97	0.37	0.34	
D33J013414.3+304228.7	20.57	22.90	0.34	0.47	
D33J013406.1+304305.4	20.60	20.61	0.29	0.22	
D33J013358.8+303928.1	20.68	21.18	0.43	0.37	
D33J013347.7+304030.9	20.69	21.34	0.40	0.39	
D33J013341.9+304021.1	20.89	...	0.33	...	
D33J013410.2+304107.1	20.90	21.04	0.32	0.38	
D33J013413.6+303939.4	20.90	21.41	0.42	0.20	
D33J013400.8+304339.9	21.05	20.99	0.28	0.26	
D33J013359.8+304725.3	21.06	22.70	0.40	0.85	
D33J013349.0+303906.2	21.12	...	0.87	...	
D33J013346.7+304210.5	21.13	...	0.96	...	(1)
D33J013412.3+304551.0	21.16	21.96	0.41	0.38	
D33J013402.1+304038.3	21.19	...	0.35	...	
D33J013349.2+303909.7	21.20	22.25	0.77	0.42	
D33J013419.5+304151.9	21.21	...	0.38	...	
D33J013357.0+304044.2	21.24	22.41	0.83	0.46	
D33J013348.5+304015.0	21.25	21.98	0.85	0.31	
D33J013405.3+303954.2	21.32	22.65	0.40	0.65	
D33J013345.1+304715.3	21.38	...	0.77	...	(1)
D33J013413.3+303848.2	21.38	21.57	0.60	0.37	
D33J013416.4+304045.9	21.41	22.50	0.78	0.34	
D33J013343.4+304248.4	21.43	22.61	0.66	0.43	
D33J013357.2+304523.0	21.47	22.25	0.43	0.66	
D33J013412.7+304208.4	21.52	...	0.52	...	(1)

Table 7. CONTINUED

Name	\bar{V}	\bar{B}	A_V	B_V	Comments
D33J013414.5+304040.4	21.56	...	0.59	...	
D33J013407.7+303845.5	21.63	...	0.81	...	
D33J013341.7+304145.7	
D33J013345.5+303912.2	
D33J013346.1+303917.7	
D33J013351.5+304050.9	
D33J013352.4+304501.7	
D33J013357.6+303844.0	
D33J013406.0+304006.0	
D33J013414.2+304740.3	...	22.19	...	0.52	

Note. — (1) Variables identified by Macri et al. (2001a)